



Design, synthesis and biological evaluation of selective histone deacetylase 6 (HDAC6) inhibitors bearing benzoindazole or pyrazoloindazole scaffold as surface recognition motif

Qihao Xu^{a,1}, Yanhua Mou^{b,1}, Siyuan Wang^a, Xiaoxiao Gao^c, Yulong Zhang^a, Zhi Wang^a, Xiangwei Xu^a, Yu Han^a, Wenlong Jia^a, Meihui Zhang^a, Linxiang Zhao^{a,*}, Dan Liu^{a,*}

^a Key Laboratory of Structure-Based Drugs Design & Discovery of Ministry of Education, Shenyang Pharmaceutical University, Shenyang 110016, China

^b Department of Pharmacology, Shenyang Pharmaceutical University, Shenyang 110016, China

^c Department of Pharmacology, Wuyi College of Innovation, Shenyang Pharmaceutical University, Shenyang 110016, China

ARTICLE INFO

Keywords:

HDAC6

Inflammatory

Neuroprotective

ABSTRACT

A series of compounds were designed and synthesized based on the compound **11i** bearing phenylpyrazole scaffold with histone deacetylase 6 (HDAC6) inhibitory activity. Most of the compounds showed considerable inhibitory activity against HDAC6 and compound **A16** with good inhibitory activity was found therein. We further found that **A16** had an inhibitory effect on inflammatory mediators (NO, TNF- α , IL-6) involved in inflammatory response and neuroendocrine regulation. In addition, **A16** has a certain neuroprotective effect on PC12 cells injured by hydrogen peroxide. Acute toxicity assay showed that the LD₅₀ of **A16** was 274.47 mg/kg in mouse model. Furthermore, **A16** displayed good stability properties in microsomes and plasma.

1. Introduction

To date, eighteen mammalian histone deacetylase (HDAC) subtypes have been identified. They are divided into four classes based on their homology to yeast original enzymes, of which class I, class II and class IV are classic zinc-dependent HDAC families [1,2]; while class III is nicotinamide adenine-dinucleotide dependent HDAC family. In class II, there are IIa and IIb subclasses. HDAC6 belongs to the HDAC IIb subclass and consists of 1215 amino acids.

Many reports have shown that the dysfunction of HDAC6 is associated with several pathology in the central nervous system [3,4]. One of the common neurological diseases is stroke, caused by the loss of local nerve function due to impaired blood circulation resulting in cell death in the brain. Some researchers have proved that the expression of HDAC6 was significantly up-regulated in both *in vitro* and *in vivo* ischemic models. They actively introduced HDAC6 inhibitors into the field of prevention and treatment for ischemic stroke. The perturbation of HDAC6 in injured brain tissue resulting in increased level of histone acetylation significantly reduced the area of cerebral infarction and neuronal apoptosis [4,5]. In the late stage of ischemic stroke, HDAC6

inhibitors can stimulate the secretion of neurotrophic factors, helping neurons and synapses remodeling, promoting nerve and angiogenesis of ischemic tissue, and promoting regeneration and repair of damaged tissue [6]. Notably, the selective inhibitors to HDAC6 are more effective for ischemic stroke and less side effects than broad-spectrum HDACs inhibitors [7].

At present, there are many HDAC6 inhibitors have been reported, and some have entered the clinical research, such as ACY-1215, ACY-241, KA2507, etc. But the inhibitors reported have not shown high selectivity, also showed a certain degree of side effects. ACY-1215, studying in clinical phase II, is only used in anti-tumor applications with low selectivity [8–12]. Although the indications of HDAC6 inhibitors in clinical research have not been applied to neuroprotection or inflammation research, HDAC6 has an important role in neuroprotection that cannot be ignored, which has been reported in many literatures [13–16].

In our previous work, the compound **11i** bearing phenylpyrazole scaffold was found [17], whose IC₅₀ against HDAC6 was 20 nM. The selective factor (SF) for HDAC1 (IC₅₀ = 2.02 μ M) was 101. SF represents the selectivity of the compound to HDAC6, and its value is the ratio of

* Corresponding authors.

E-mail addresses: linxiang.zhao@vip.sina.com (L. Zhao), sammyld@163.com (D. Liu).

¹ These authors contributed equally to this work.

the IC_{50} of HDAC1 to HDAC6. The larger the value, the higher the selectivity. The result of molecular docking of **11i** and HDAC6 showed that the surface recognition moiety (SRM) of **11i** interacted with the amino acid residues **Pro501**, **Phe620**, **Phe680** and **His651** of the hydrophobic pocket of HDAC6 protein (Fig. 1).

In order to increase interaction between the SRM of **11i** and HDAC6, the volume of SRM of **11i** was increased through the conformation constrained strategy, then the four compounds with benzindazole (**A1-A4**) were designed and synthesized (Fig. 2).

In addition, **TS-15**, bearing isoxazoloindazole scaffold, was also obtained in the previous work, whose IC_{50} against HDAC6 was 9 nM. The SF for HDAC1 ($IC_{50} = 0.59 \mu M$) was 65. We combined **11i** and **TS-15** for superimposed molecular docking and found that the part of SRM in the two compounds could occupy the hydrophobic region of the entire protein (Fig. 3). Therefore, we combined the SRM regions of the two compounds to obtain a series of compounds bearing pyrazoloindazole scaffold (Fig. 4).

2. Results and discussion

2.1. Chemistry

Using 6-methoxy-1-naphthylketone (**1-1**) or 1-tetralone (**3-1**) as the starting material, a condensation reaction with appropriate acyl chloride yields an intermediate **1-2-4-2**. Then, a cyclization reaction with hydrazine hydrate is carried out to construct a key intermediate **1-3-4-3** with benzindazole scaffold. Nucleophilic substitution reaction with a halide, an ammonolysis reaction of ester with aqueous hydroxylamine solution get the final target compound **A1-A4** (Scheme 1).

With 1,3-cyclohexanedione as the starting material, it was reacted

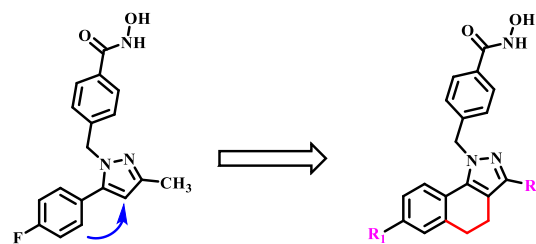


Fig. 2. The design strategy of compounds A1-A4.

with DMF-DMA (*N,N*-dimethylformamide dimethyl acetal) and hydrazine hydrochloride to obtain the key intermediate **M2**. The nuclear substitution reaction yields intermediates **5-1**, **7-1**, **9-1**, **11-1**, and then condensation reaction with appropriate acyl chloride, cyclization reaction with hydrazine hydrate construct the key intermediates **5-3-12-3**, **17-3-19-3** bearing pyrazoloindazole scaffold. Nucleophilic substitution reaction with halogenated compounds, ammonolysis reaction of esters with hydroxylamine aqueous solution obtain target compounds **A5-A34** (Scheme 2).

2.2. Biological activity

2.2.1. Enzyme activity test of the compounds in vitro

Since the hit compounds **11i** and **TS-15** had no enzyme inhibitory activity on HDAC8 and HDAC11 at the maximum tested concentration (HDAC8, **11i**, $IC_{50} > 5 \mu M$, **TS-15**, $IC_{50} > 10 \mu M$; HDAC11, **TS-15**, $IC_{50} > 10 \mu M$), we mainly performed HDAC1, 2, 3 and 6 enzyme activity tests on the compounds. **Tubacin** and **ACY-1215** were used as positive controls. The results indicated that all the compounds showed certain inhibitory activity against HDAC6, and the IC_{50} ranged from 2.2 nM to 550 nM. Among them, **A12**, **A17**, **A19**, **A20**, **A21**, **A23** and **A30** had single digit nanomole inhibitory activity against HDAC6, and their inhibitory activity was also better than that of **ACY-1215** (Tables 1 and 2).

Based on the enzyme activity results, we could roughly summarize the preliminary structure-activity relationship (SAR): **a**. When the tricyclic system was pyrazoloindazole, the enzyme activity was better; **b**. In the target compounds with pyrazoloindazole as SRM, the order in which the R_1 substituents affect the inhibitory activity of HDAC6 was: $6-CH_2CH_2OCH_3 > 7-CH_2CH_2OCH_3 > 7-CH_3 > 7-CH_2CH_3$; the order in which the R_2 substituents affect the inhibitory activity of HDAC6 was: $-CH_3 > -Ph > -Bn$; **c**. When a vinyl group was inserted into the linker, the inhibitory activity of most compounds on HDAC6 was reduced. According to the summarized SAR, we obtained compound **A16** with good HDAC6 inhibitory activity.

2.2.2. Evaluation of inhibitory activity of compounds against NO release

The increase of NO release is one of the important signs of neuronal inflammation. Therefore, we evaluated the inhibitory activity of the compounds with good inhibitory activities against HDAC6 on the release of NO. Lipopolysaccharide (LPS) induced microglial cell inflammation model was selected (Table 3).

The results showed that all the compounds could effectively inhibit NO release. Compounds **A10**, **A16** and **A27** had better activity, and the IC_{50} value of **A16** was 0.01 μM .

2.2.3. Intra-cellular target validation

We then explored whether these compounds could inhibit HDAC6 in cellular condition. High acetylation of histone H3 was a sign of inhibition by the Class I family, and acetylation of tubulin was a sign of HDAC6 inhibition. The levels of histone H3, acetylated histone H3 and α -tubulin were determined by western blot assay in SH-SY5Y cell treated with compound **A16** at different concentration and **Tubacin** at 1 μM for 12 h. In SH-SY5Y cell line, **A16** and **Tubacin** promoted acetylation of

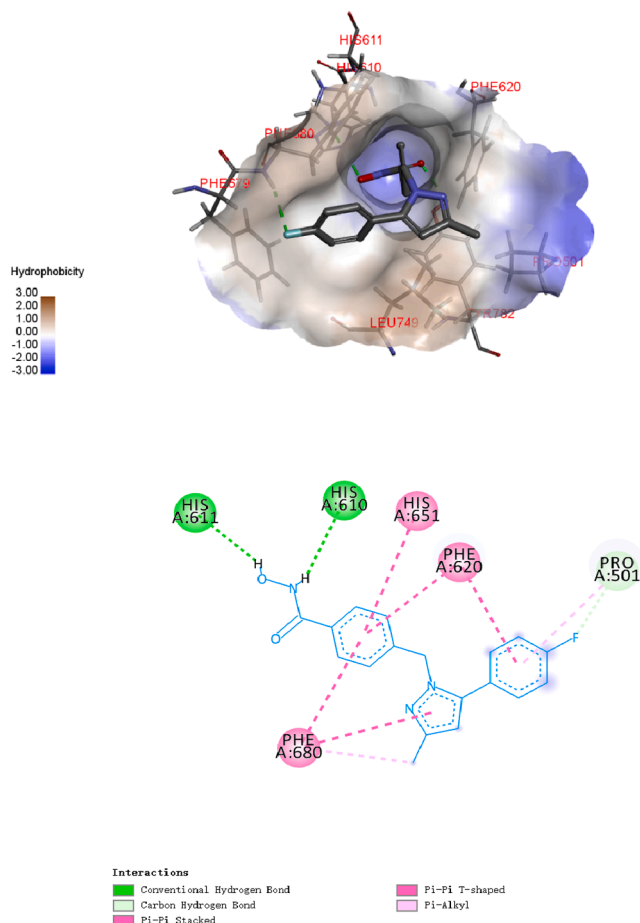


Fig. 1. The possible binding mode of **11i** to HDAC6 (PDB: 5EDU).

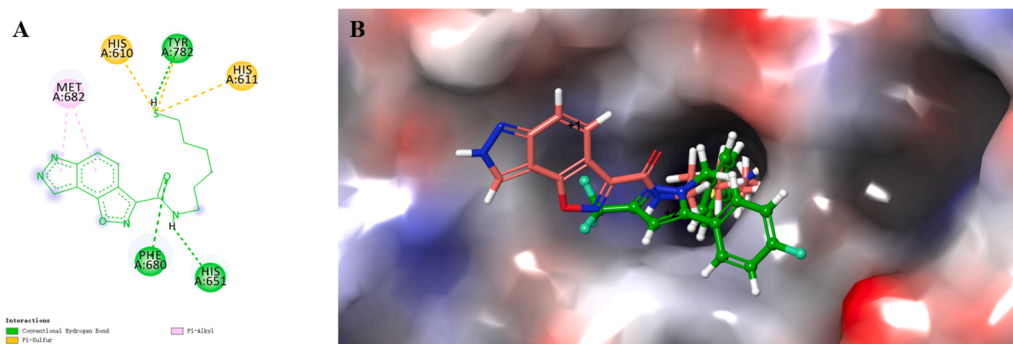


Fig. 3. The structure of TS-15, 11i (green) and TS-15 (yellow) possible binding mode to HDAC6 (PDB: 5EDU). (For interpretation of the references to colour in this figure legend, the reader is referred to the web version of this article.)

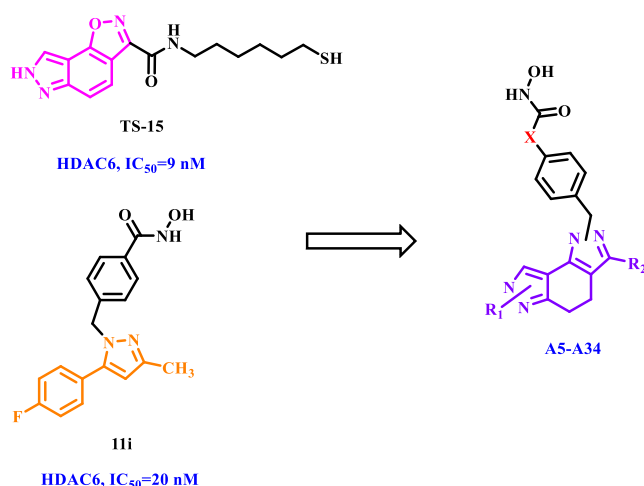


Fig. 4. The design strategy of compounds A5-A34.

α -tubulin but not histone H3, which proved that **A16** was a selective HDAC6 inhibitor. This finding was in accord with the enzyme-based assay (Fig. 5).

2.2.4. The inhibition of **A16** LPS induced release of inflammatory mediators from microglia

In the pathological mechanism of ischemic stroke, the inflammatory response played an important role. After ischemic stroke, the microglia inherent in the brain were activated [18]. Initial research suggested that microglial cell would aggravate brain tissue damage in the acute phase [19], but as the research progressed, it was found in animal models that the lack of microglial cell would affect the stability of microvascular structures, thereby further increasing ischemia injury of cerebral stroke [20]. It could be seen that microglia played a complex and important role in ischemic stroke.

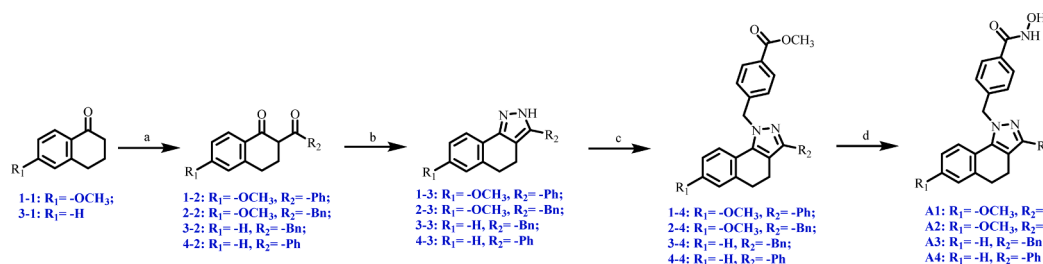
Microglia cells were treated with LPS for 24 h and the NO level in the

nutrient solution was significantly increased. On the other hand, 0.01 μ M of **A16** could effectively reduce the NO level. The positive drug ACY-1215 also showed a strong inhibitory effect on NO. In addition, **A16** can reduce the release of TNF- α and IL-6 induced by LPS, also showing a good concentration dependence. In conclusion, **A16** can generally inhibit the synthesis and release of LPS-induced inflammatory mediators. MTT results showed that 10 μ M of **A16** had certain cytotoxicity, 10 μ M of ACY-1215 also had cytotoxicity, weaker than **A16**. By using sodium nitroprusside (SNP, 25 mM) as the NO donor, it was found that **A16** and ACY-1215 could capture a certain amount of NO free radicals at 0.01 μ M and 0.1 μ M, suggesting that the effect of NO reduction was at least partly due to its direct trapping ability (Fig. 6).

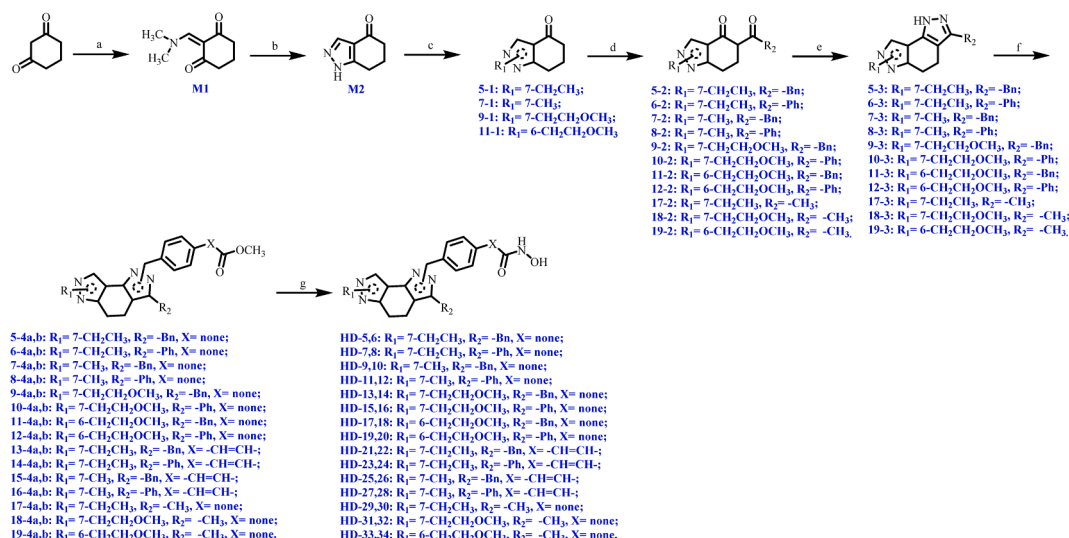
2.2.5. Evaluation of the protective effect of **A16** on H_2O_2 -induced on nerve cell line PC12

After cerebral ischemia, multiple factors such as inflammation, apoptosis, oxidative stress, and excitotoxicity interact and affect each other, thereby exacerbating the occurrence and development of nerve damage [21]. Recent studies have shown that oxidative stress plays a central role in cerebral ischemia-reperfusion injury. During cerebral ischemia, oxidative stress and its reactive oxygen species such as superoxide anion and hydroxyl radicals (reactive oxygen species) (ROS) damage is an important mechanism of acute cerebral ischemia [22,23]. So we chose a model of hydrogen peroxide-induced neuronal death.

It was investigated whether compound **A16** provided protection against neurons, in addition to inhibiting excessive activation of microglia. Using H_2O_2 -induced oxidative stress model, the cells were pre-protected with **A16** for 1 h before H_2O_2 stimulation and incubate them with H_2O_2 for 16 h. It was found that cells in the H_2O_2 group almost completely died, while 0.01 μ M **A16** could significantly improve the cell survival rate, reaching the normal level. Similarly, ACY-1215 can provide better protection. DPPH free radical scavenging experiment showed that **A16** and ACY-1215 didn't fight against oxidative stress through free radical scavenging, but were more likely mediated by biological system (Fig. 7). The specific mechanism remains to be further studied.



Scheme 1. The synthesis of A1-A4. Reagents and conditions: a. R_2COCl , LiHMDS, dry THF, N_2 , r.t., 6 h; b. $NH_2NH_2 \cdot H_2O$, AcOH, 100 $^{\circ}C$, 1 h; c. methyl 4-(bromomethyl)benzoate, K_2CO_3 , MeCN, 70 $^{\circ}C$, 4 h; d. $NH_2OH \cdot H_2O$, NaOH, MeOH, r.t., 6 h.



Scheme 2. The synthesis of A5-A34. Reagents and conditions: a. DMF-DMA, 95 °C, 1 h; b. $\text{NH}_2\text{NH}_2\text{HCl}$, MeOH, 70 °C, 3 h; c. R_1X , K_2CO_3 , MeCN, 70 °C, 4 h; d. R_2COCl , LiHMDS, dry THF, N_2 , r.t., 6 h; e. $\text{NH}_2\text{NH}_2\cdot\text{H}_2\text{O}$, AcOH, 100 °C, 1 h; f. methyl 4-(bromomethyl)benzoate or (E)-methyl 3-(4-(bromomethyl)phenyl)acrylate, K_2CO_3 , MeCN, 70 °C, 4 h; g. $\text{NH}_2\text{OH}\cdot\text{H}_2\text{O}$, NaOH, MeOH, r.t., 6 h.

Table 1

Enzyme profiles of A1-A4 against HDAC.

Compd.	R	n	IC ₅₀ (μM)			
			HDAC1	HDAC2	HDAC3	HDAC6
A1	-OCH ₃	0	>2.0	1.27	0.34	0.028
A2	-OCH ₃	1	>2.0	>2.0	0.18	0.25
A3	-H	1	0.27	>2.0	0.27	0.086
A4	-H	0	>2.0	>2.0	0.30	0.12
11i	-	-	2.021	1.974	1.205	0.020
TS-15	-	-	0.588	0.151	0.229	0.009
Tubacin	-	-	1.56	1.37	0.48	0.016
ACY-1215	-	-	0.10	0.066	0.037	0.009

Values were the mean of two independent determinations.

2.2.6. The stability assay of A16

To provide some basic information on drug-like properties, metabolic stability studies of compounds A16 was assessed in liver microsomes of human and rat, Midazolam was used as a reference compound. As shown in Table 4, A16 displayed relative stable metabolic stabilities with $T_{1/2}$ of 113.61 and 82.50 min in human and rat liver microsomes, respectively. In addition, A16 stabilities in rat plasma were assessed. To our delight, compound A16 was very stable in rat plasma during the whole incubation time (see Table 5).

2.2.7. Acute toxicity assay of compound A16

In order to evaluate the toxicity of A16, acute toxicity assay was conducted. Five dose groups of Kunming male mice were designed, each group of 3 animals, grouped as follows, 1000 mg/kg, 500 mg/kg, 250 mg/kg, 125 mg/kg, 62.5 mg/kg. It was administered at a maximum administration volume of 0.1 ml/10 g by intraperitoneal injection (i.p.). Fully dissolved before drug administration. After drug administration, the mice closed their eyes and drooped, their activities were significantly reduced, and their actions were especially slow. Their fur was dull, not smooth, and their spirits were poor. No animals died on the day of administration.

Using the CFDA chemical drug standard method Bliss to calculate. From the data analysis, the LD₅₀ of compound A16 in Kunming male

mice was 274.47 mg/kg, and the 95% confidence limit of LD₅₀ was 184.56–408.17 mg/kg.

The organs of the dead mice were biopsied with doses of 500 mg/kg and 1000 mg/kg. Observation results of pathological sections by hematoxylin-eosin (HE) staining showed that the dose at 500 mg/kg had a certain effect on the heart of mice. The pathological sections showed that the muscle septum was widened, the red blood cells were hemorrhagic, and a few inflammatory cells were also visible, while the rest of the organs were normal (Fig. 8).

The dose at 1000 mg/kg did some damage to the liver of mice. Tissue sections showed that the liver was slightly turbid and swollen, while other organs were normal (Fig. 9).

3. Conclusion

In order to develop potent and neuroprotective selective HDAC6 inhibitor, using 11i as the hit compound, 34 compounds bearing benzimidazole or pyrazolindazole scaffold were designed and synthesized through the conformational restriction strategy. By analyzing the results of enzyme activity and cell activity *in vitro*, a better active compound A16 was obtained. Compound A16 can have a certain inhibitory effect on some inflammatory mediators (NO, TNF-α, IL-6), which is equivalent to the positive control drug ACY-1215. In addition, it has been observed that the drug has a direct neurocyte protective effect. Both A16 and ACY-1215 can protect PC12 cell death caused by hydrogen peroxide. Acute toxicity assay results of A16 show that when the doses reach 500 mg/kg and 1000 mg/kg, respectively, it has a certain effect on the heart and liver of mice, and the LD₅₀ value is 274.47 mg/kg. The stability results of A16 show that the drug has good metabolic stability *in vitro*. The above experimental results show that HDAC6 plays an important role in the nervous system, especially in stroke, cerebral ischemia and some neuroinflammation. Small molecule HDAC6 inhibitors have certain development value in these aspects.

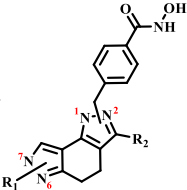
4. Experimental

4.1. Chemistry

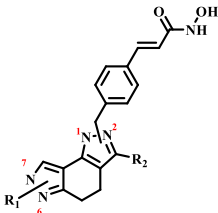
All starting materials and solvents were obtained from commercial suppliers or prepared according to known procedures without further purification. Tubacin was purchased from Bidepharm (Shanghai, China; CAS: 537049-40-4) with a purity of 95%. All reactions were monitored

Table 2

Enzyme profiles of A5-A34 against HDAC.



Compd.	R ₁	R ₂	Position	IC ₅₀ (μM)			
				HDAC1	HDAC2	HDAC3	HDAC6
A5	7-C ₂ H ₅	-Bn	1	0.28	>2.0	0.28	0.35
A6	7-C ₂ H ₅	-Bn	2	>2.0	0.42	0.16	0.16
A7	7-C ₂ H ₅	-Ph	1	0.19	0.40	0.24	0.15
A8	7-C ₂ H ₅	-Ph	2	>2.0	>2.0	0.12	0.048
A9	7-CH ₃	-Bn	1	0.095	>2.0	0.11	0.25
A10	7-CH ₃	-Bn	2	0.40	1.18	0.10	0.014
A11	7-CH ₃	-Ph	1	0.15	0.99	0.39	0.053
A12	7-CH ₃	-Ph	2	0.22	>2.0	0.094	0.0022
A13	7-C ₂ H ₄ OCH ₃	-Bn	1	>2.0	>2.0	0.74	0.11
A14	7-C ₂ H ₄ OCH ₃	-Bn	2	0.81	0.69	0.49	0.24
A15	7-C ₂ H ₄ OCH ₃	-Ph	1	1.01	0.81	0.45	0.12
A16	7-C ₂ H ₄ OCH ₃	-Ph	2	0.43	>2.0	0.20	0.011
A17	6-C ₂ H ₄ OCH ₃	-Bn	1	0.78	>2.0	0.54	0.0044
A18	6-C ₂ H ₄ OCH ₃	-Bn	2	0.82	>2.0	0.65	0.31
A19	6-C ₂ H ₄ OCH ₃	-Ph	1	0.34	0.28	0.093	0.0064
A20	6-C ₂ H ₄ OCH ₃	-Ph	2	0.29	0.41	0.10	0.0078
A29	7-C ₂ H ₅	-CH ₃	1	0.12	1.65	0.36	0.063
A30	7-C ₂ H ₅	-CH ₃	2	0.16	0.14	0.019	0.004
A31	7-C ₂ H ₄ OCH ₃	-CH ₃	1	0.12	0.73	0.47	0.12
A32	7-C ₂ H ₄ OCH ₃	-CH ₃	2	0.25	0.10	0.0038	0.016
A33	6-C ₂ H ₄ OCH ₃	-CH ₃	1	>2.0	>2.0	>2.0	0.30
A34	6-C ₂ H ₄ OCH ₃	-CH ₃	2	>2.0	>2.0	>2.0	0.073
11i	-	-	-	2.021	1.974	1.205	0.020
TS-15	-	-	-	0.588	0.151	0.229	0.009
Tubacin	-	-	-	1.56	1.37	0.48	0.016
ACY-1215	-	-	-	0.10	0.066	0.037	0.009



Compd.	R ₁	R ₂	Position	IC ₅₀ (μM)			
				HDAC1	HDAC2	HDAC3	HDAC6
A21	7-C ₂ H ₅	-Bn	1	>2.0	0.30	0.090	0.0078
A22	7-C ₂ H ₅	-Bn	2	0.34	1.20	0.17	0.31
A23	7-C ₂ H ₅	-Ph	1	0.83	0.16	0.057	0.0081
A24	7-C ₂ H ₅	-Ph	2	0.32	>2.0	0.14	0.21
A25	7-CH ₃	-Bn	1	0.18	0.11	0.048	0.16
A26	7-CH ₃	-Bn	2	>2.0	0.77	0.17	0.55
A27	7-CH ₃	-Ph	1	0.55	0.23	0.073	0.14
A28	7-CH ₃	-Ph	2	0.39	0.71	0.11	0.085
11i	-	-	-	2.021	1.974	1.205	0.020
TS-15	-	-	-	0.588	0.151	0.229	0.009
Tubacin	-	-	-	1.56	1.37	0.48	0.016
ACY-1215	-	-	-	0.10	0.066	0.037	0.009

Values were the mean of two independent determinations.

Table 3

The anti-NO release activities of indicated compounds.

Compd.	IC ₅₀ (μM)	Compd.	IC ₅₀ (μM)
A8	0.292	A21	0.115
A10	0.085	A23	0.117
A12	0.823	A27	0.026
A16	0.010	A30	0.775
A19	0.635	A32	0.666
A20	0.593	Minocycline	16.28

Values were the mean of two independent determinations

by thin-layer chromatography (TLC), using silica gel plates with fluorescence F254 and ultraviolet (UV) light visualization (Qingdao Haiyang Chemical, China). Column chromatography was conducted for compounds purification using silica gel (200–300 mesh). The melting points (M.p.) were taken on an electrically heated X4 digital visual melting point apparatus and were uncorrected. ¹H NMR and ¹³C NMR were generated in DMSO-*d*₆ on Bruker spectrometers (600 MHz), using TMS as internal standard. LC-MS data were recorded on an Agilent 1100 Series LC/MSD Trap using ESI mode. High-resolution mass spectra (HRMS) were performed on Agilent 6540 UHD accurate mass Q-TOF MS

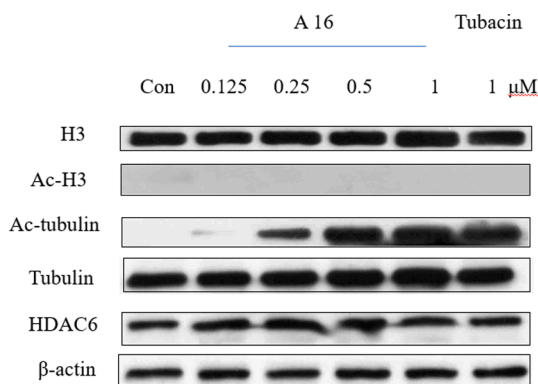


Fig. 5. Validation of HDAC6 inhibition in SH-SY5Y cells after 12 h of treatment with compound A16 at 0.125, 0.25, 0.5, 1 μM and Tubacin at 1 μM.

in ESI mode with Agilent 1290 infinity HPLC. All the target compounds were characterized by ^1H NMR, ^{13}C NMR, LC-MS and HRMS.

4.1.1. General procedure for the synthesis of A1-A4

Material **1-1** (0.5 g, 2.84 mmol) was dissolved in 40 ml THF, adding lithium bis(trimethylsilyl)amide (5.7 ml, 5.68 mmol) at 0 °C. Benzoyl chloride (0.4 ml, 3.41 mmol) was added into the mixture at the same temperature. The mixture was stirred at room temperature for 6 h. The resulting solution was dried directly in vacuum to give **1-2** as yellow solid.

To a solution of **1-2** in 50 ml acetic acid was added 80% hydrazine hydrate (0.23 ml, 3.58 mmol). The reaction was warmed to 100 °C for 1 h. 150 ml water was added into the resulting solution, and extracted with ethyl acetate (30 ml \times 3). The organic layers were combined, washed with saturated sodium bicarbonate, dried with Na_2SO_4 and evaporated. Finally, the resulting residue was purified by column chromatography on silica gel as indicated to give **1-3** as white solid.

To a solution of **1-3** (0.3 g, 1.09 mmol) in 50 ml acetonitrile was added methyl 4-(bromomethyl)benzoate (0.5 g, 2.18 mmol) and K_2CO_3

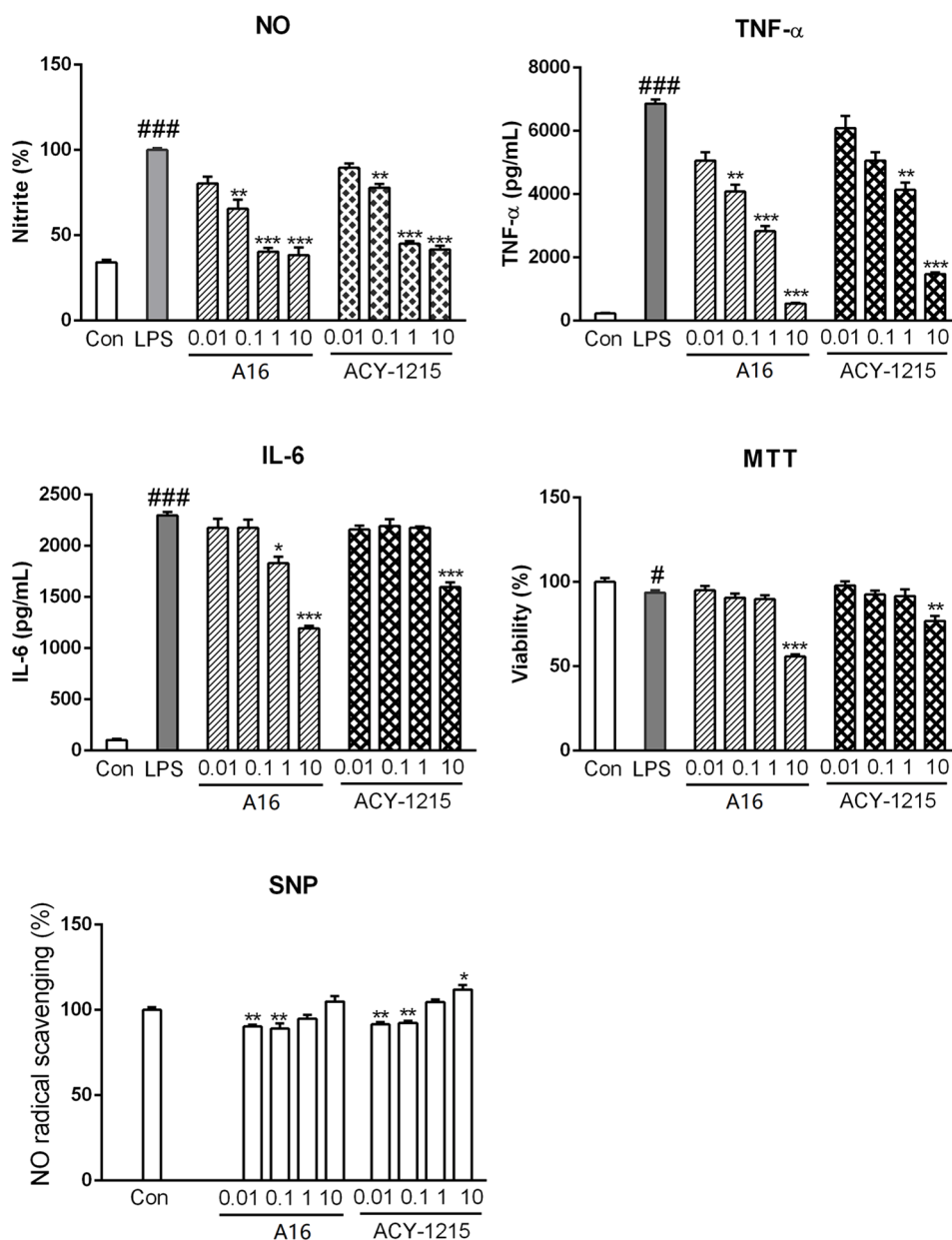


Fig. 6. The decrease LPS-induced inflammatory mediator release of A16 and ACY-1215 in N9 microglia cells. NO: compound A16 decreased LPS-induced NO release. Compound A16 decreased LPS-induced TNF- α (TNF- α) and IL-6 (IL-6) production in N9 microglia. MTT: The effect of compound A16 and ACY-1215 on cell viability. SNP: compound A16 had NO radical scavenging activity. Data were shown as mean \pm SD. # p < 0.05, ### p < 0.001 compared with control group and * p < 0.05, ** p < 0.01 and *** p < 0.001 compared with model group.

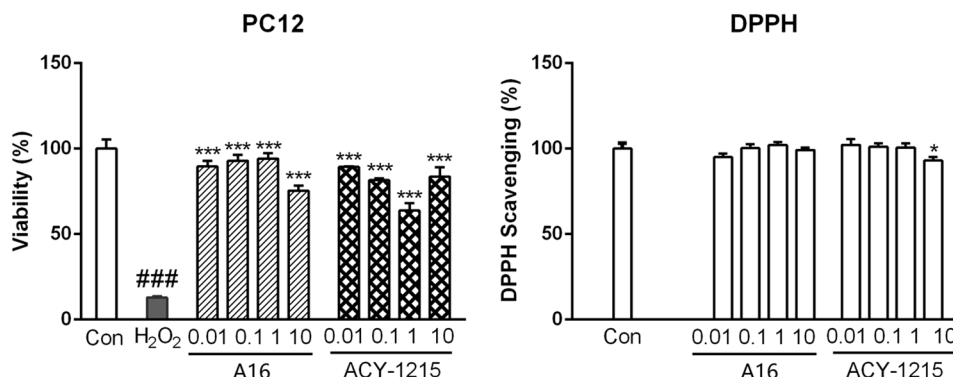


Fig. 7. The H₂O₂-induced cell death protection of A16 and ACY-1215 in PC12 cells. MTT: PC12 cells were pre-treated with A16 and ACY-1215 for 1 h, and then H₂O₂ was added and incubated for 16 h. Cells were added with 5 mg/ml MTT and incubated for additional 4 h. Data were shown as mean \pm SD. ### $p < 0.001$ compared with control group and *** $p < 0.001$ compared with H₂O₂ group. DPPH: A16 had no DPPH free radical scavenging activity. * $p < 0.05$ compared with control group.

Table 4
The metabolic stability study of A16.

Compd.	Species	T _{1/2} (minute)	Cl _{int} (mL/min/kg)
A16	Human	113.61	15.30
	Rat	82.50	30.11
Midazolam	Human	6.35	273.91
	Rat	2.56	969.83

Values were the mean of two independent determinations.

Table 5
The stability study of A16 in rat plasma.

Compd.	Species	T _{1/2} (minute)
A16	Rat	>120

Values were the mean of two independent determinations.

(0.27 g, 2.18 mmol). The reaction was warmed to 70 °C for 4 h. Finally, the resulting residue was purified by column chromatography on silica gel as indicated to give **1-4** as white solid.

To a solution of **1-4** (0.2 g, 0.47 mmol) in methanol (20 ml) was added NaOH (2 mol/L, 4 ml) and NH₂OH (50 wt% in water, 3 ml) dropwise successively at 0 °C. The reaction was warmed to room temperature for 6 h. The mixture solution was concentrated to dryness, and the obtained solid was dissolved in water (10 ml). The resulting solution was adjusted to neutral with 1 mol/L aqueous solution of HCl. Finally, the resulting residue was purified by column chromatography on silica gel as indicated to give **A1** as white solid.

Compounds **A2-A4** were synthesized by the synthetic method from **1** to **1** to **A1** as white solid.

4.1.1.1. N-hydroxy-4-[(7-methoxy-3-phenyl-4,5-dihydro-1H-benzo[g]indazol-2-yl)methyl]benzamide (A1). Yield: 53.1%. Mp: 194–197 °C. ESI-MS: m/z , 424.3 [M–H][−]. ¹H NMR (600 MHz, DMSO-*d*₆) δ : 11.16 (s, 1H), 9.02 (s, 1H), 7.63 (d, J = 8.0 Hz, 2H), 7.46–7.42 (m, 5H), 7.39–7.30 (m, 3H), 7.07 (d, J = 8.1 Hz, 2H), 5.39 (s, 2H), 3.77 (s, 3H), 2.90 (t, J = 7.9 Hz, 2H), 2.67 (t, J = 8.1 Hz, 2H). ¹³C NMR (151 MHz, DMSO) δ : 164.2, 159.1, 147.3, 146.4, 141.6, 141.2, 139.8, 138.6, 133.8, 132.2, 129.9, 129.3, 129.0, 127.5, 127.1, 126.9, 123.4, 119.6, 115.2, 114.6, 114.3, 112.7, 55.5, 29.7, 20.5, 19.3. HRMS (ESI+) m/z calcd for C₂₆H₂₃N₃O₃ [M–H][−] 424.1739 found: 424.1654.

4.1.1.2. N-hydroxy-4-[(3-benzyl-7-methoxy-4,5-dihydro-1H-benzo[g]indazol-2-yl)methyl]benzamide (A2). Yield: 26.1%. Mp: 108–113 °C. ESI-MS: m/z , 438.3 [M–H][−]. ¹H NMR (600 MHz, DMSO-*d*₆) δ : 11.14 (s, 1H), 9.00 (s, 1H), 7.63 (d, J = 8.0 Hz, 2H), 7.28 (d, J = 7.1 Hz, 2H), 7.13–7.08 (m, 5H), 6.92–6.75 (m, 3H), 5.30 (s, 2H), 4.01 (s, 2H), 3.76 (s, 3H), 2.84 (t, J = 7.3 Hz, 2H), 2.55 (t, J = 7.4 Hz, 2H). ¹³C NMR (151 MHz, DMSO) δ : 164.2, 158.9, 146.9, 140.3, 139.4, 138.4, 137.6, 128.9, 128.7, 127.4,

127.2, 126.7, 126.5, 126.3, 119.9, 115.7, 115.2, 114.3, 112.6, 112.0, 55.4, 52.2, 32.7, 30.9, 29.7, 19.0. HRMS (ESI+) m/z calcd for C₂₇H₂₅N₃O₃ [M–H][−] 438.1896 found: 438.1821.

4.1.1.3. N-hydroxy-4-[(3-benzyl-4,5-dihydro-1H-benzo[g]indazol-2-yl)methyl]benzamide (A3). Yield: 38.7%. Mp: 140–144 °C. ESI-MS: m/z , 408.1 [M–H][−]. ¹H NMR (600 MHz, DMSO-*d*₆) δ : 11.15 (s, 1H), 9.01 (s, 1H), 7.66–7.62 (m, 2H), 7.26 (m, 2H), 7.24–7.14 (m, 5H), 7.14–7.08 (m, 4H), 5.33 (s, 2H), 4.03 (s, 2H), 2.86 (t, J = 7.3 Hz, 2H), 2.57 (t, J = 8.1 Hz, 2H). ¹³C NMR (151 MHz, DMSO) δ : 164.2, 146.9, 141.2, 138.3, 137.8, 137.3, 136.6, 132.1, 130.1, 128.9, 128.7, 127.4, 127.2, 127.0, 126.8, 126.5, 121.9, 115.2, 54.0, 52.3, 32.6, 29.3, 18.9. HRMS (ESI+) m/z calcd for C₂₆H₂₃N₃O₂ [M–H][−] 408.1790 found: 408.1699.

4.1.1.4. N-hydroxy-4-[(3-phenyl-4,5-dihydro-1H-benzo[g]indazol-2-yl)methyl]benzamide (A4). Yield: 42.2%. Mp: 187–192 °C. ESI-MS: m/z , 394.3 [M–H][−]. ¹H NMR (600 MHz, DMSO-*d*₆) δ : 11.18 (s, 1H), 9.06 (s, 1H), 7.71–7.69 (m, 2H), 7.50–7.45 (m, 5H), 7.40–7.36 (m, 4H), 7.21–7.18 (m, 2H), 5.81 (s, 2H), 2.92 (t, J = 8.2 Hz, 2H), 2.69 (t, J = 7.3 Hz, 2H). ¹³C NMR (151 MHz, DMSO) δ : 163.0, 146.3, 145.5, 138.9, 138.1, 136.5, 135.8, 132.7, 128.4, 128.3, 128.0, 127.1, 126.9, 126.1, 125.5, 121.5, 115.4, 53.4, 51.7, 29.6, 28.3, 19.4, 18.2. HRMS (ESI+) m/z calcd for C₂₅H₂₁N₃O₂ [M–H][−] 394.1634 found: 394.1567.

4.1.2. Procedure for the synthesis of 1,5,6,7-tetrahydro-4H-indazol-4-one (M2)

Material **1,3-Cyclohexanedione** (10.0 g, 89.2 mmol) was dissolved in 30 ml **N,N**-dimethylformamide dimethyl acetal (DMF-DMA). The reaction was warmed to 95 °C for 1 h. The resulting solution was dried directly in vacuum to give **M1** as reddish brown solid.

To a solution of **M1** (14.9 g) in 150 ml methanol was added hydrazine hydrochloride (11.2 g, 107.0 mmol). The reaction was warmed to 65 °C for 3 h. The resulting solution was dried directly in vacuum to give the yellow solid. The solid was dripped washing with 60 ml dichloromethane and dried to give **M2** as yellowish solid.

4.1.3. General procedure for the synthesis of A5-A34

To a solution of **M2** (5.8 g, 42.6 mmol) in 150 ml acetonitrile was added EtBr (6.4 ml, 85.2 mmol) and K₂CO₃ (11.8 g, 85.2 mmol). The reaction was warmed to 70 °C for 4 h. Finally, the resulting residue was purified by column chromatography on silica gel as indicated to give **5-1** as yellowish solid.

Material **5-1** (0.5 g, 3.0 mmol) was dissolved in 50 ml THF, adding lithium bis(trimethylsilyl)amide (6.0 ml, 6.0 mmol) at 0 °C. Phenylacetyl chloride (0.8 ml, 4.5 mmol) was added into the mixture at the same temperature. The mixture was stirred at room temperature for 6 h. The resulting solution was dried directly in vacuum to give **5-2** as yellow solid.

To a solution of **5-2** in 50 ml acetic acid was added 80% hydrazine hydrate (0.25 ml, 5.0 mmol). The reaction was warmed to 100 °C for 1 h.

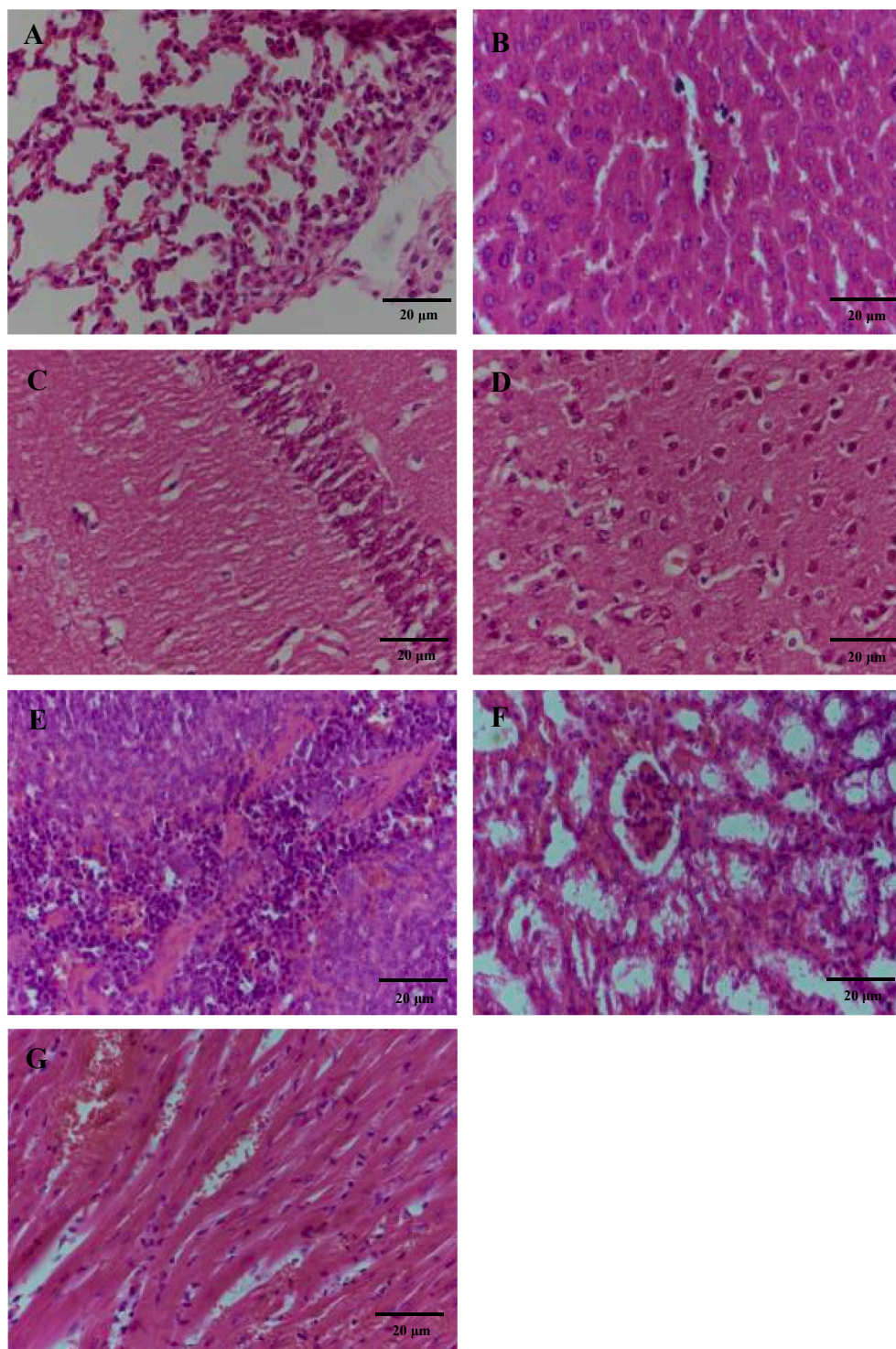


Fig. 8. The effect of dosage of 500 mg/kg on pathology of mouse organs (400 magnification). Scale bar = 20 μm . (A) lung; (B) liver; (C) brain (hippocampus); (D) brain; (E) spleen; (F) kidney; (G) heart.

150 ml water was added into the resulting solution, and extracted with ethyl acetate (30 ml \times 3). The organic layers were combined, washed with saturated sodium bicarbonate, dried with Na_2SO_4 and evaporated. Finally, the resulting residue was purified by column chromatography on silica gel as indicated to give **5-3** as white solid.

To a solution of **5-3** (0.4 g, 1.4 mmol) in 50 ml acetonitrile was added methyl 4-(bromomethyl)benzoate (0.48 g, 2.1 mmol) and K_2CO_3 (0.34 g, 2.8 mmol). The reaction was warmed to 70 $^\circ\text{C}$ for 4 h. Finally, the resulting residue was purified by column chromatography on silica gel

as indicated to give **5-4a** and **5-4b** as white solid.

To a solution of **5-4a** (0.08 g, 0.19 mmol) or **5-4b** (0.08 g, 0.19 mmol) in methanol (10 ml) was added NaOH (2 mol/L, 3 ml) and NH_2OH (50 wt% in water, 2 ml) dropwise successively at 0 $^\circ\text{C}$. The reaction was warmed to room temperature for 6 h. The mixture solution was concentrated to dryness, and the obtained solid was dissolved in water (10 ml). The resulting solution was adjusted to neutral with 1 mol/L aqueous solution of HCl. Finally, the resulting residue was purified by column chromatography on silica gel as indicated to give **A5** or

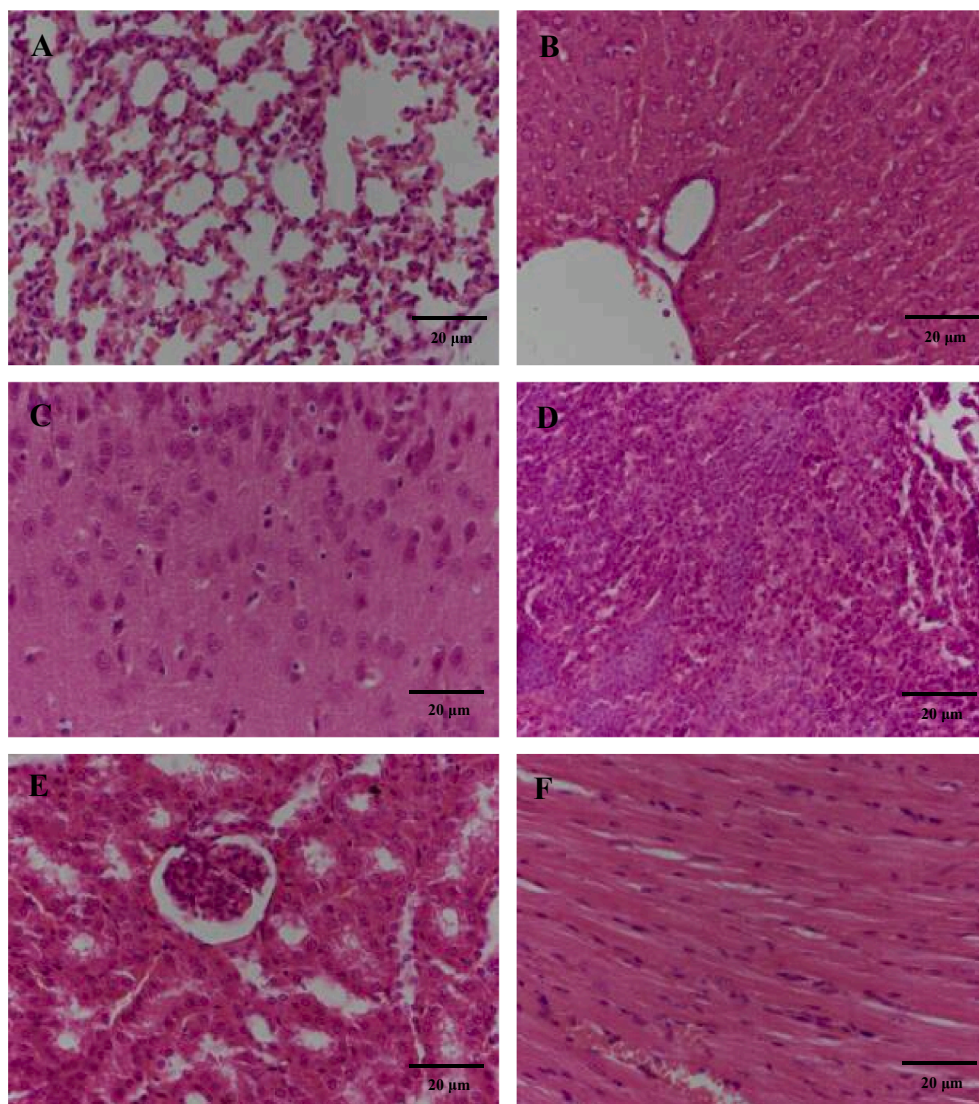


Fig. 9. The effect of dosage of 1000 mg/kg on pathology of mouse organs (400 magnification). Scale bar = 20 µm. (A) lung; (B) liver; (C) brain; (D) spleen; (E) kidney; (F) heart.

A6 as white solid.

Compounds **A7–A34** were synthesized by the synthetic method from **M2** to **A5** or **A6** as white solid.

4.1.3.1. N-hydroxy-4-[(3-benzyl-7-ethyl-4,5-dihydropyrazolo[3,4-*e*]indazol-1(7*H*)-yl)methyl]benzamide (A5). Yield: 1.1%. Mp: 135–138 °C. ESI-MS: m/z , 425.9 $[M-H]^-$. 1H NMR (600 MHz, DMSO- d_6) δ : 11.18 (s, 1H), 9.01 (s, 1H), 7.95 (s, 1H), 7.68 (d, $J = 8.0$ Hz, 2H), 7.26 (d, $J = 7.3$ Hz, 2H), 7.24–7.13 (m, 5H), 5.41 (s, 2H), 4.04 (q, $J = 7.2$ Hz, 2H), 3.88 (s, 2H), 2.69 (t, $J = 7.4$ Hz, 2H), 2.55 (t, $J = 7.7$ Hz, 2H), 1.33 (t, $J = 7.2$ Hz, 3H). ^{13}C NMR (151 MHz, DMSO) δ : 149.4, 147.7, 140.3, 135.2, 128.8, 128.7, 127.2, 126.2, 123.0, 111.9, 108.2, 52.7, 46.5, 32.9, 22.0, 19.5, 15.8. HRMS (ESI+) m/z calcd for $C_{25}H_{25}N_5O_2$ $[M-H]^-$ 426.2008 found: 426.1924.

4.1.3.2. N-hydroxy-4-[(3-benzyl-7-ethyl-4,5-dihydropyrazolo[3,4-*e*]indazol-2(7*H*)-yl)methyl]benzamide (A6). Yield: 1.2%. Mp: 132–136 °C. ESI-MS: m/z , 426.4 $[M-H]^-$. 1H NMR (600 MHz, DMSO- d_6) δ : 11.12 (s, 1H), 9.01 (s, 1H), 7.95 (s, 1H), 7.68 (d, $J = 7.9$ Hz, 2H), 7.26 (d, $J = 7.4$ Hz, 2H), 7.24–7.14 (m, 5H), 5.42 (s, 2H), 4.04 (q, $J = 7.3$ Hz, 2H), 3.88 (s, 2H), 2.69 (t, $J = 7.7$ Hz, 2H), 2.55 (t, $J = 7.9$ Hz, 2H), 1.33 (t, $J = 7.2$ Hz, 3H). ^{13}C NMR (151 MHz, DMSO) δ : 164.3, 149.4, 147.7, 141.3, 140.3,

135.2, 132.3, 128.8, 128.7, 127.5, 127.2, 126.2, 123.0, 112.0, 108.2, 52.7, 46.5, 32.9, 22.0, 19.5, 15.8. HRMS (ESI+) m/z calcd for $C_{25}H_{25}N_5O_2$ $[M-H]^-$ 426.2008 found: 426.1938.

4.1.3.3. N-hydroxy-4-[(7-ethyl-3-phenyl-4,5-dihydropyrazolo[3,4-*e*]indazol-1(7*H*)-yl)methyl]benzamide (A7). Yield: 1.5%. Mp: 164–166 °C. ESI-MS: m/z , 412.3 $[M-H]^-$. 1H NMR (600 MHz, DMSO- d_6) δ : 11.15 (s, 1H), 8.93 (s, 1H), 8.03 (s, 1H), 7.70 (d, $J = 6.1$ Hz, 2H), 7.68 (d, $J = 6.8$ Hz, 2H), 7.47–7.24 (m, 5H), 5.52 (s, 2H), 4.09 (q, $J = 7.2$ Hz, 2H), 2.99 (t, $J = 7.6$ Hz, 2H), 2.81 (t, $J = 7.6$ Hz, 2H), 1.36 (t, $J = 7.2$ Hz, 3H). ^{13}C NMR (151 MHz, DMSO) δ : 163.6, 149.4, 147.2, 136.0, 134.2, 128.9, 127.6, 127.5, 127.3, 127.0, 123.4, 114.1, 111.3, 108.0, 53.1, 46.6, 22.2, 20.8, 15.9. HRMS (ESI+) m/z calcd for $C_{24}H_{23}N_5O_2$ $[M-H]^-$ 412.1852 found: 412.1746.

4.1.3.4. N-hydroxy-4-[(7-ethyl-3-phenyl-4,5-dihydropyrazolo[3,4-*e*]indazol-2(7*H*)-yl)methyl]benzamide (A8). Yield: 1.8%. Mp: 205–207 °C. ESI-MS: m/z , 412.3 $[M-H]^-$. 1H NMR (600 MHz, DMSO- d_6) δ : 11.14 (s, 1H), 9.00 (s, 1H), 7.89 (s, 1H), 7.64 (d, $J = 8.0$ Hz, 2H), 7.47–7.37 (m, 5H), 7.04 (d, $J = 7.9$ Hz, 2H), 5.31 (s, 2H), 4.10 (q, $J = 7.2$ Hz, 2H), 2.76 (d, $J = 5.9$ Hz, 2H), 2.72 (d, $J = 6.0$ Hz, 2H), 1.38 (t, $J = 7.2$ Hz, 3H). ^{13}C NMR (151 MHz, DMSO) δ : 164.3, 149.8, 143.9, 141.7, 139.9, 132.1, 130.0,

129.3, 128.9, 127.4, 126.9, 123.3, 113.6, 111.3, 52.4, 46.5, 22.1, 19.8, 16.0. HRMS (ESI+) m/z calcd for $C_{24}H_{23}N_5O_2$ [M-H]⁻ 412.1852 found: 412.1756.

4.1.3.5. N-hydroxy-4-[(3-benzyl-7-methyl-4,5-dihydropyrazolo[3,4-*e*]indazol-1(7*H*)-yl)methyl]benzamide (A9). Yield: 2.9%. Mp: 162–167 °C. ESI-MS: m/z , 412.3 [M-H]⁻. ¹H NMR (600 MHz, DMSO-*d*₆) δ: 11.14 (s, 1H), 9.01 (s, 1H), 7.90 (s, 1H), 7.67 (d, *J* = 8.1 Hz, 2H), 7.27 (t, *J* = 7.5 Hz, 2H), 7.23–7.19 (m, 4H), 7.17 (t, *J* = 7.3 Hz, 1H), 5.41 (s, 2H), 3.88 (s, 2H), 3.75 (s, 3H), 2.68 (t, *J* = 7.6 Hz, 2H), 2.55 (t, *J* = 7.6 Hz, 2H). ¹³C NMR (151 MHz, DMSO) δ: 164.5, 149.7, 147.8, 141.2, 140.1, 135.1, 132.1, 128.8, 128.7, 127.5, 127.2, 126.3, 124.4, 114.2, 112.1, 108.3, 52.7, 38.7, 32.8, 21.8, 19.4. HRMS (ESI+) m/z calcd for $C_{24}H_{23}N_5O_2$ [M-H]⁻ 412.1852 found: 412.1764.

4.1.3.6. N-hydroxy-4-[(3-benzyl-7-methyl-4,5-dihydropyrazolo[3,4-*e*]indazol-2(7*H*)-yl)methyl]benzamide (A10). Yield: 3.7%. Mp: 158–160 °C. ESI-MS: m/z , 412.4 [M-H]⁻. ¹H NMR (600 MHz, DMSO-*d*₆) δ: 11.15 (s, 1H), 9.00 (s, 1H), 7.75 (s, 1H), 7.62 (d, *J* = 8.1 Hz, 2H), 7.25 (t, *J* = 7.5 Hz, 2H), 7.18 (t, *J* = 7.3 Hz, 1H), 7.11 (d, *J* = 7.4 Hz, 2H), 7.06 (d, *J* = 8.1 Hz, 2H), 5.24 (s, 2H), 4.00 (s, 2H), 3.79 (s, 3H), 2.71 (t, *J* = 7.3 Hz, 2H), 2.61 (t, *J* = 7.2 Hz, 2H). ¹³C NMR (151 MHz, DMSO) δ: 164.5, 150.0, 143.3, 141.4, 138.3, 137.8, 131.9, 128.9, 128.6, 127.3, 126.8, 124.5, 113.3, 111.6, 52.1, 38.6, 29.8, 21.9, 19.3. HRMS (ESI+) m/z calcd for $C_{24}H_{23}N_5O_2$ [M-H]⁻ 412.1852 found: 412.1759.

4.1.3.7. N-hydroxy-4-[(7-methyl-3-phenyl-4,5-dihydropyrazolo[3,4-*e*]indazol-1(7*H*)-yl)methyl]benzamide (A11). Yield: 2.6%. Mp: 148–152 °C. ESI-MS: m/z , 397.7 [M-H]⁻. ¹H NMR (600 MHz, DMSO-*d*₆) δ: 11.14 (s, 1H), 9.02 (s, 1H), 7.98 (s, 1H), 7.69 (t, *J* = 8.5 Hz, 4H), 7.43 (t, *J* = 7.7 Hz, 2H), 7.33 (t, *J* = 7.4 Hz, 1H), 7.28 (d, *J* = 8.3 Hz, 2H), 5.52 (s, 2H), 3.80 (s, 3H), 2.99 (t, *J* = 7.6 Hz, 2H), 2.80 (t, *J* = 7.6 Hz, 2H). ¹³C NMR (151 MHz, DMSO) δ: 164.3, 149.6, 147.3, 140.8, 136.0, 134.2, 132.4, 128.9, 127.6, 127.3, 127.0, 124.7, 111.3, 108.1, 53.0, 22.1, 20.8. HRMS (ESI+) m/z calcd for $C_{23}H_{21}N_5O_2$ [M-H]⁻ 398.1695 found: 398.1622.

4.1.3.8. N-hydroxy-4-[(7-methyl-3-phenyl-4,5-dihydropyrazolo[3,4-*e*]indazol-2(7*H*)-yl)methyl]benzamide (A12). Yield: 5.7%. Mp: 155–158 °C. ESI-MS: m/z , 397.7 [M-H]⁻. ¹H NMR (600 MHz, DMSO-*d*₆) δ: 11.15 (s, 1H), 9.00 (s, 1H), 7.84 (s, 1H), 7.64 (d, *J* = 8.3 Hz, 2H), 7.49 (t, *J* = 7.3 Hz, 2H), 7.44 (t, *J* = 7.9 Hz, 1H), 7.39–7.36 (m, 2H), 7.04 (d, *J* = 8.3 Hz, 2H), 5.31 (s, 2H), 3.81 (s, 3H), 2.75 (t, *J* = 6.6 Hz, 2H), 2.70 (t, *J* = 6.8 Hz, 2H). ¹³C NMR (151 MHz, DMSO) δ: 164.3, 150.0, 143.8, 139.9, 132.1, 130.0, 129.3, 129.3, 128.9, 127.5, 126.9, 124.7, 113.6, 111.5, 52.4, 38.8, 22.0, 19.8. HRMS (ESI+) m/z calcd for $C_{23}H_{21}N_5O_2$ [M-H]⁻ 398.1695 found: 398.1591.

4.1.3.9. N-hydroxy-4-[(3-benzyl-7-(2-methoxyethyl)-4,5-dihydropyrazolo[3,4-*e*]indazol-1(7*H*)-yl)methyl]benzamide (A13). Yield: 1.0%. Mp: 145–148 °C. ESI-MS: m/z , 455.8 [M-H]⁻. ¹H NMR (600 MHz, DMSO-*d*₆) δ: 11.15 (s, 1H), 9.03 (s, 1H), 7.90 (s, 1H), 7.68 (d, *J* = 8.0 Hz, 2H), 7.27 (t, *J* = 7.5 Hz, 2H), 7.21 (d, *J* = 7.6 Hz, 4H), 7.17 (t, *J* = 7.2 Hz, 1H), 5.41 (s, 2H), 4.16 (t, *J* = 5.1 Hz, 2H), 3.89 (s, 2H), 3.63 (t, *J* = 5.2 Hz, 2H), 3.18 (s, 3H), 2.69 (t, *J* = 7.5 Hz, 2H), 2.55 (t, *J* = 7.6 Hz, 2H). ¹³C NMR (151 MHz, DMSO) δ: 164.5, 149.6, 147.7, 141.2, 140.3, 135.1, 132.3, 128.8, 128.7, 127.5, 127.2, 126.2, 124.3, 112.0, 108.2, 70.7, 58.3, 52.7, 51.4, 32.9, 22.0, 19.4. HRMS (ESI+) m/z calcd for $C_{26}H_{27}N_5O_3$ [M-H]⁻ 456.2114 found: 456.2036.

4.1.3.10. N-hydroxy-4-[(3-benzyl-7-(2-methoxyethyl)-4,5-dihydropyrazolo[3,4-*e*]indazol-2(7*H*)-yl)methyl]benzamide (A14). Yield: 0.7%. Mp: 161–166 °C. ESI-MS: m/z , 455.8 [M-H]⁻. ¹H NMR (600 MHz, DMSO-*d*₆) δ: 11.15 (s, 1H), 9.00 (s, 1H), 7.76 (s, 1H), 7.62 (d, *J* = 7.8 Hz, 2H), 7.25 (t, *J* = 7.3 Hz, 2H), 7.18 (t, *J* = 7.2 Hz, 1H), 7.11 (d, *J* = 7.5 Hz,

2H), 7.05 (d, *J* = 7.9 Hz, 2H), 5.23 (s, 2H), 4.20 (t, *J* = 5.2 Hz, 2H), 4.00 (s, 2H), 3.66 (t, *J* = 5.2 Hz, 2H), 3.23 (s, 3H), 2.73 (t, *J* = 7.3 Hz, 2H), 2.62 (t, *J* = 7.3 Hz, 2H). ¹³C NMR (151 MHz, DMSO) δ: 149.9, 143.3, 138.4, 137.6, 128.9, 128.6, 128.5, 127.2, 126.7, 125.0, 124.2, 114.0, 113.2, 111.6, 70.9, 58.3, 52.0, 51.2, 29.8, 22.1, 19.4. HRMS (ESI+) m/z calcd for $C_{26}H_{27}N_5O_3$ [M-H]⁻ 456.2114 found: 456.2030.

4.1.3.11. N-hydroxy-4-[(7-(2-methoxyethyl)-3-phenyl-4,5-dihydropyrazolo[3,4-*e*]indazol-1(7*H*)-yl)methyl]benzamide (A15). Yield: 0.8%. Mp: 202–208 °C. ESI-MS: m/z , 441.9 [M-H]⁻. ¹H NMR (600 MHz, DMSO-*d*₆) δ: 11.14 (s, 1H), 9.01 (s, 1H), 7.99 (s, 1H), 7.69 (t, *J* = 7.5 Hz, 4H), 7.44 (t, *J* = 7.5 Hz, 2H), 7.33 (t, *J* = 7.3 Hz, 1H), 7.28 (d, *J* = 7.9 Hz, 2H), 5.53 (s, 2H), 4.20 (t, *J* = 5.1 Hz, 2H), 3.67 (t, *J* = 5.1 Hz, 2H), 3.21 (s, 3H), 2.99 (t, *J* = 7.5 Hz, 2H), 2.81 (t, *J* = 7.6 Hz, 2H). ¹³C NMR (151 MHz, DMSO) δ: 149.6, 149.5, 148.5, 147.2, 146.5, 135.9, 135.3, 134.4, 134.2, 128.9, 128.9, 128.6, 127.3, 127.0, 127.0, 114.1, 111.4, 111.1, 108.3, 108.0, 70.7, 58.3, 53.1, 51.4, 22.1, 20.8. HRMS (ESI+) m/z calcd for $C_{25}H_{25}N_5O_3$ [M-H]⁻ 442.1957 found: 442.1894.

4.1.3.12. N-hydroxy-4-[(7-(2-methoxyethyl)-3-phenyl-4,5-dihydropyrazolo[3,4-*e*]indazol-2(7*H*)-yl)methyl]benzamide (A16). Yield: 0.6%. Mp: 191–193 °C. ESI-MS: m/z , 441.8 [M-H]⁻. ¹H NMR (600 MHz, DMSO-*d*₆) δ: 11.15 (s, 1H), 8.99 (s, 1H), 7.85 (s, 1H), 7.64 (d, *J* = 7.8 Hz, 2H), 7.49 (t, *J* = 7.4 Hz, 2H), 7.44 (t, *J* = 7.0 Hz, 1H), 7.38 (d, *J* = 7.9 Hz, 2H), 7.04 (d, *J* = 7.9 Hz, 2H), 5.32 (s, 2H), 4.23 (t, *J* = 5.1 Hz, 2H), 3.68 (t, *J* = 5.1 Hz, 2H), 3.25 (s, 3H), 2.77 (t, *J* = 7.2 Hz, 2H), 2.72 (t, *J* = 7.0 Hz, 2H). ¹³C NMR (151 MHz, DMSO) δ: 164.3, 150.1, 143.8, 141.7, 139.9, 132.1, 130.0, 129.3, 128.9, 127.5, 126.9, 124.5, 113.6, 111.3, 70.9, 58.3, 52.4, 51.3, 22.1, 19.8. HRMS (ESI+) m/z calcd for $C_{25}H_{25}N_5O_3$ [M-H]⁻ 442.1957 found: 442.1877.

4.1.3.13. N-hydroxy-4-[(3-benzyl-6-(2-methoxyethyl)-4,5-dihydropyrazolo[3,4-*e*]indazol-1(6*H*)-yl)methyl]benzamide (A17). Yield: 0.7%. Mp: 159–164 °C. ESI-MS: m/z , 456.0 [M-H]⁻. ¹H NMR (600 MHz, DMSO-*d*₆) δ: 11.14 (s, 1H), 9.00 (s, 1H), 7.67 (d, *J* = 8.0 Hz, 2H), 7.60 (s, 1H), 7.28 (t, *J* = 7.5 Hz, 2H), 7.23 (t, *J* = 6.4 Hz, 4H), 7.18 (t, *J* = 6.5 Hz, 1H), 5.47 (s, 2H), 4.18 (t, *J* = 5.0 Hz, 2H), 3.89 (s, 2H), 3.60 (t, *J* = 5.0 Hz, 2H), 3.16 (s, 3H), 2.82 (t, *J* = 8.0 Hz, 2H), 2.57 (t, *J* = 7.9 Hz, 2H). ¹³C NMR (151 MHz, DMSO) δ: 164.4, 147.5, 141.4, 141.1, 140.3, 135.6, 132.3, 132.0, 130.0, 128.8, 128.7, 127.5, 127.1, 126.3, 110.4, 108.9, 71.0, 58.4, 52.9, 49.1, 33.0, 20.5, 19.1. HRMS (ESI+) m/z calcd for $C_{26}H_{27}N_5O_3$ [M-H]⁻ 456.2114 found: 456.2034.

4.1.3.14. N-hydroxy-4-[(3-benzyl-6-(2-methoxyethyl)-4,5-dihydropyrazolo[3,4-*e*]indazol-2(6*H*)-yl)methyl]benzamide (A18). Yield: 0.5%. Mp: 202–204 °C. ESI-MS: m/z , 455.9 [M-H]⁻. ¹H NMR (600 MHz, DMSO-*d*₆) δ: 11.18 (s, 1H), 9.00 (s, 1H), 7.63 (d, *J* = 8.2 Hz, 2H), 7.54 (s, 1H), 7.25 (t, *J* = 7.5 Hz, 2H), 7.18 (t, *J* = 7.3 Hz, 1H), 7.12 (d, *J* = 7.3 Hz, 2H), 7.06 (d, *J* = 8.2 Hz, 2H), 5.23 (s, 2H), 4.22 (t, *J* = 5.3 Hz, 2H), 4.00 (s, 2H), 3.64 (t, *J* = 5.3 Hz, 2H), 3.20 (s, 3H), 2.86 (t, *J* = 7.6 Hz, 2H), 2.65 (t, *J* = 7.6 Hz, 2H). ¹³C NMR (151 MHz, DMSO) δ: 164.2, 143.7, 141.2, 138.4, 137.6, 132.3, 128.9, 128.6, 127.4, 127.2, 126.7, 112.1, 71.2, 58.5, 51.9, 48.9, 29.9, 20.4, 19.0. HRMS (ESI+) m/z calcd for $C_{26}H_{27}N_5O_3$ [M-H]⁻ 456.2114 found: 456.2028.

4.1.3.15. N-hydroxy-4-[(6-(2-methoxyethyl)-3-phenyl-4,5-dihydropyrazolo[3,4-*e*]indazol-1(6*H*)-yl)methyl]benzamide (A19). Yield: 0.7%. Mp: 130–134 °C. ESI-MS: m/z , 442.0 [M-H]⁻. ¹H NMR (600 MHz, DMSO-*d*₆) δ: 11.14 (s, 1H), 9.01 (s, 1H), 7.69 (m, 5H), 7.44 (t, *J* = 7.5 Hz, 2H), 7.33 (t, *J* = 7.3 Hz, 1H), 7.30 (d, *J* = 7.9 Hz, 2H), 5.58 (s, 2H), 4.24 (t, *J* = 5.0 Hz, 2H), 3.64 (t, *J* = 5.1 Hz, 2H), 3.19 (s, 3H), 3.03 (t, *J* = 7.7 Hz, 2H), 2.95 (t, *J* = 7.8 Hz, 2H). ¹³C NMR (151 MHz, DMSO) δ: 147.0, 141.3, 136.4, 134.3, 132.2, 128.9, 127.6, 127.2, 127.0, 109.8, 108.7, 71.0, 58.5, 53.3, 49.2, 20.7, 20.5. HRMS (ESI+) m/z calcd for $C_{25}H_{25}N_5O_3$ [M-H]⁻ 442.1957 found: 442.1875.

4.1.3.16. *N*-hydroxy-4-[(6-(2-methoxyethyl)-3-phenyl-4,5-dihydropyrazolo[3,4-*e*]indazol-2(7*H*)-yl)methyl]benzamide (A20). Yield: 0.5%. Mp: 159–166 °C. ESI-MS: *m/z*, 441.8 [M–H][–]. ¹H NMR (600 MHz, DMSO-*d*₆) δ: 11.15 (s, 1H), 8.99 (s, 1H), 7.67–7.60 (m, 3H), 7.49 (t, *J* = 7.4 Hz, 2H), 7.44 (t, *J* = 7.1 Hz, 1H), 7.38 (d, *J* = 7.5 Hz, 2H), 7.04 (d, *J* = 8.0 Hz, 2H), 5.31 (s, 2H), 4.24 (t, *J* = 5.0 Hz, 2H), 3.65 (t, *J* = 5.0 Hz, 2H), 3.20 (s, 3H), 2.91 (t, *J* = 7.5 Hz, 2H), 2.76 (t, *J* = 7.6 Hz, 2H). ¹³C NMR (151 MHz, DMSO) δ: 164.3, 144.3, 141.8, 141.4, 139.8, 132.5, 132.1, 130.1, 129.3, 128.9, 127.5, 126.8, 112.3, 111.9, 71.2, 58.5, 52.4, 48.9, 29.1, 20.5, 19.4. HRMS (ESI+) *m/z* calcd for C₂₅H₂₅N₅O₃ [M–H][–] 442.1957 found: 442.1865.

4.1.3.17. (*E*)-*N*-hydroxy-3-{4-[(3-benzyl-7-ethyl-4,5-dihydropyrazolo[3,4-*e*]indazol-1(7*H*)-yl)methyl]phenyl}acrylamide (A21). Yield: 9.5%. Mp: 164–168 °C. ESI-MS: *m/z*, 452.3 [M–H][–]. ¹H NMR (600 MHz, DMSO-*d*₆) δ: 10.76 (s, 1H), 9.03 (s, 1H), 7.94 (s, 1H), 7.50 (d, *J* = 8.1 Hz, 3H), 7.42 (d, *J* = 15.8 Hz, 1H), 7.27 (t, *J* = 7.5 Hz, 3H), 7.17 (m, 3H), 6.42 (d, *J* = 15.8 Hz, 1H), 5.39 (s, 2H), 4.05 (q, *J* = 7.3 Hz, 2H), 3.88 (s, 2H), 2.69 (t, *J* = 7.6 Hz, 2H), 2.54 (t, *J* = 7.6 Hz, 2H), 1.33 (t, *J* = 7.2 Hz, 3H). ¹³C NMR (151 MHz, DMSO) δ: 163.0, 149.4, 147.6, 140.3, 139.5, 135.2, 134.3, 128.8, 128.7, 128.1, 127.8, 126.2, 123.0, 119.4, 111.9, 108.2, 52.7, 46.5, 32.9, 22.0, 19.5, 15.8. HRMS (ESI+) *m/z* calcd for C₂₇H₂₇N₅O₂ [M–H][–] 452.2165 found: 452.2079.

4.1.3.18. (*E*)-*N*-hydroxy-3-{4-[(3-benzyl-7-ethyl-4,5-dihydropyrazolo[3,4-*e*]indazol-2(7*H*)-yl)methyl]phenyl}acrylamide (A22). Yield: 3.7%. Mp: 206–208 °C. ESI-MS: *m/z*, 452.3 [M–H][–]. ¹H NMR (600 MHz, DMSO-*d*₆) δ: 10.75 (s, 1H), 9.02 (s, 1H), 7.81 (s, 1H), 7.44 (d, *J* = 8.0 Hz, 2H), 7.40 (d, *J* = 15.8 Hz, 1H), 7.24 (t, *J* = 7.5 Hz, 2H), 7.18 (d, *J* = 7.2 Hz, 1H), 7.11 (d, *J* = 7.3 Hz, 2H), 7.03 (d, *J* = 8.0 Hz, 2H), 6.40 (d, *J* = 15.8 Hz, 1H), 5.21 (s, 2H), 4.08 (q, *J* = 7.2 Hz, 2H), 4.00 (s, 2H), 2.72 (t, *J* = 7.3 Hz, 2H), 2.61 (t, *J* = 7.3 Hz, 2H), 1.36 (t, *J* = 7.2 Hz, 3H). ¹³C NMR (151 MHz, DMSO) δ: 163.1, 149.7, 143.3, 139.7, 138.4, 138.3, 137.5, 134.2, 128.9, 128.6, 127.9, 126.7, 123.0, 119.3, 113.2, 111.6, 52.1, 46.4, 29.8, 22.2, 19.4, 16.0. HRMS (ESI+) *m/z* calcd for C₂₇H₂₇N₅O₂ [M–H][–] 452.2165 found: 452.2099.

4.1.3.19. (*E*)-*N*-hydroxy-3-{4-[(7-ethyl-3-phenyl-4,5-dihydropyrazolo[3,4-*e*]indazol-1(7*H*)-yl)methyl]phenyl}acrylamide (A23). Yield: 6.9%. Mp: 168–170 °C. ESI-MS: *m/z*, 438.3 [M–H][–]. ¹H NMR (600 MHz, DMSO-*d*₆) δ: 10.74 (s, 1H), 9.02 (s, 1H), 8.03 (s, 1H), 7.68 (d, *J* = 7.2 Hz, 2H), 7.52 (d, *J* = 8.1 Hz, 2H), 7.42 (m, 3H), 7.32 (m, 1H), 7.27 (d, *J* = 8.1 Hz, 2H), 6.42 (d, *J* = 15.8 Hz, 1H), 5.50 (s, 2H), 4.09 (q, *J* = 7.2 Hz, 2H), 2.99 (t, *J* = 7.6 Hz, 2H), 2.81 (t, *J* = 7.6 Hz, 2H), 1.37 (t, *J* = 7.3 Hz, 3H). ¹³C NMR (151 MHz, DMSO) δ: 163.0, 149.4, 147.2, 139.1, 136.0, 134.2, 128.9, 128.1, 127.9, 127.6, 127.0, 123.4, 119.5, 111.3, 108.0, 53.1, 46.6, 22.2, 20.8, 15.9. HRMS (ESI+) *m/z* calcd for C₂₆H₂₅N₅O₂ [M–H][–] 438.2008 found: 438.1928.

4.1.3.20. (*E*)-*N*-hydroxy-3-{4-[(7-ethyl-3-phenyl-4,5-dihydropyrazolo[3,4-*e*]indazol-2(7*H*)-yl)methyl]phenyl}acrylamide (A24). Yield: 4.0%. Mp: 164–168 °C. ESI-MS: *m/z*, 438.3 [M–H][–]. ¹H NMR (600 MHz, DMSO-*d*₆) δ: 10.75 (s, 1H), 9.02 (s, 1H), 7.89 (s, 1H), 7.46 (m, 5H), 7.39 (t, 3H), 7.01 (d, *J* = 8.1 Hz, 2H), 6.40 (d, *J* = 15.8 Hz, 1H), 5.29 (s, 2H), 4.10 (q, *J* = 7.2 Hz, 2H), 2.76 (t, *J* = 6.7 Hz, 2H), 2.71 (t, *J* = 6.8 Hz, 2H), 1.38 (t, *J* = 7.2 Hz, 3H). ¹³C NMR (151 MHz, DMSO) δ: 163.2, 149.9, 143.8, 139.9, 138.4, 134.1, 130.0, 129.3, 128.9, 128.0, 127.5, 123.3, 119.3, 113.6, 111.3, 52.5, 46.5, 22.1, 19.8, 16.0. HRMS (ESI+) *m/z* calcd for C₂₆H₂₅N₅O₂ [M–H][–] 438.2008 found: 438.1921.

4.1.3.21. (*E*)-*N*-hydroxy-3-{4-[(3-benzyl-7-methyl-4,5-dihydropyrazolo[3,4-*e*]indazol-1(7*H*)-yl)methyl]phenyl}acrylamide (A25). Yield: 2.5%. Mp: 165–168 °C. ESI-MS: *m/z*, 438.4 [M–H][–]. ¹H NMR (600 MHz, DMSO-*d*₆) δ: 10.78 (s, 1H), 9.02 (s, 1H), 7.90 (s, 1H), 7.50 (d, *J* = 7.8 Hz, 2H), 7.40 (d, *J* = 16.0 Hz, 1H), 7.27 (t, *J* = 5.7 Hz, 2H), 7.22 (t, *J* = 6.1

Hz, 2H), 7.20–7.16 (m, 3H), 6.43 (d, *J* = 15.6 Hz, 1H), 5.38 (s, 2H), 3.87 (s, 2H), 3.76 (s, 3H), 2.68 (t, *J* = 7.5 Hz, 2H), 2.56 (t, *J* = 7.3 Hz, 2H). ¹³C NMR (151 MHz, DMSO) δ: 163.2, 149.7, 147.7, 140.1, 139.4, 138.4, 135.1, 134.3, 128.8, 128.7, 128.1, 127.7, 126.3, 124.4, 119.2, 112.0, 108.3, 52.7, 38.7, 32.8, 21.8, 19.4. HRMS (ESI+) *m/z* calcd for C₂₆H₂₅N₅O₂ [M–H][–] 438.2008 found: 438.1926.

4.1.3.22. (*E*)-*N*-hydroxy-3-{4-[(3-benzyl-7-methyl-4,5-dihydropyrazolo[3,4-*e*]indazol-2(7*H*)-yl)methyl]phenyl}acrylamide (A26). Yield: 2.3%. Mp: 188–190 °C. ESI-MS: *m/z*, 438.3 [M–H][–]. ¹H NMR (600 MHz, DMSO-*d*₆) δ: 10.74 (s, 1H), 9.02 (s, 1H), 7.75 (s, 1H), 7.43 (d, *J* = 7.8 Hz, 2H), 7.39 (d, *J* = 15.7 Hz, 1H), 7.24 (t, *J* = 5.6 Hz, 2H), 7.18 (t, *J* = 7.2 Hz, 1H), 7.11 (d, *J* = 7.5 Hz, 2H), 7.03 (d, *J* = 7.8 Hz, 2H), 6.40 (d, *J* = 15.8 Hz, 1H), 5.21 (s, 2H), 4.00 (s, 2H), 3.79 (s, 3H), 2.71 (t, *J* = 5.3 Hz, 2H), 2.60 (t, *J* = 5.3 Hz, 2H). ¹³C NMR (151 MHz, DMSO) δ: 163.1, 149.9, 143.2, 139.7, 138.4, 137.5, 134.2, 128.9, 128.6, 127.9, 126.7, 124.4, 119.3, 113.2, 111.8, 52.1, 38.7, 29.8, 22.1, 19.4. HRMS (ESI+) *m/z* calcd for C₂₆H₂₅N₅O₂ [M–H][–] 438.2008 found: 438.1905.

4.1.3.23. (*E*)-*N*-hydroxy-3-{4-[(7-methyl-3-phenyl-4,5-dihydropyrazolo[3,4-*e*]indazol-1(7*H*)-yl)methyl]phenyl}acrylamide (A27). Yield: 2.9%. Mp: 201–204 °C. ESI-MS: *m/z*, 423.7 [M–H][–]. ¹H NMR (600 MHz, DMSO-*d*₆) δ: 10.76 (s, 1H), 9.12 (s, 1H), 7.98 (s, 1H), 7.68 (d, *J* = 7.4 Hz, 2H), 7.52 (d, *J* = 7.9 Hz, 2H), 7.43 (t, *J* = 7.6 Hz, 2H), 7.38 (d, *J* = 15.8 Hz, 1H), 7.33 (t, *J* = 7.3 Hz, 1H), 7.25 (d, *J* = 7.9 Hz, 2H), 6.41 (d, *J* = 15.8 Hz, 1H), 5.49 (s, 2H), 3.80 (s, 3H), 2.98 (t, *J* = 7.6 Hz, 2H), 2.80 (t, *J* = 7.6 Hz, 2H). ¹³C NMR (151 MHz, DMSO) δ: 162.9, 149.6, 147.2, 139.0, 135.9, 134.2, 128.9, 128.1, 127.9, 127.6, 127.0, 124.7, 119.5, 111.3, 108.2, 53.1, 38.8, 22.1, 20.8. HRMS (ESI+) *m/z* calcd for C₂₅H₂₃N₅O₂ [M–H][–] 424.1852 found: 424.1768.

4.1.3.24. (*E*)-*N*-hydroxy-3-{4-[(7-methyl-3-phenyl-4,5-dihydropyrazolo[3,4-*e*]indazol-2(7*H*)-yl)methyl]phenyl}acrylamide (A28). Yield: 4.7%. Mp: 181–186 °C. ESI-MS: *m/z*, 423.7 [M–H][–]. ¹H NMR (600 MHz, DMSO-*d*₆) δ: 10.78 (s, 1H), 9.02 (s, 1H), 7.84 (s, 1H), 7.51–7.42 (m, 6H), 7.38 (d, *J* = 7.0 Hz, 2H), 7.01 (d, *J* = 7.9 Hz, 2H), 6.42 (d, *J* = 15.8 Hz, 1H), 5.28 (s, 2H), 3.81 (s, 3H), 2.75 (t, *J* = 6.5 Hz, 2H), 2.70 (t, *J* = 6.7 Hz, 2H). ¹³C NMR (151 MHz, DMSO) δ: 163.1, 150.0, 143.7, 139.8, 138.2, 134.2, 130.0, 129.3, 129.3, 128.9, 128.0, 127.5, 124.7, 119.4, 113.6, 111.5, 52.5, 38.8, 22.0, 19.8. HRMS (ESI+) *m/z* calcd for C₂₅H₂₃N₅O₂ [M–H][–] 424.1852 found: 424.1770.

4.1.3.25. *N*-hydroxy-4-[(7-ethyl-3-methyl-4,5-dihydropyrazolo[3,4-*e*]indazol-1(7*H*)-yl)methyl]benzamide (A29). Yield: 3.2%. Mp: 137–140 °C. ESI-MS: *m/z*, 350.2 [M–H][–]. ¹H NMR (600 MHz, DMSO-*d*₆) δ: 11.14 (s, 1H), 9.00 (s, 1H), 7.94 (s, 1H), 7.67 (d, *J* = 8.1 Hz, 2H), 7.20 (d, *J* = 8.1 Hz, 2H), 5.36 (s, 2H), 4.05 (q, *J* = 7.1 Hz, 2H), 2.74 (t, *J* = 7.6 Hz, 2H), 2.65 (t, *J* = 7.4 Hz, 2H), 2.10 (s, 3H), 1.34 (t, *J* = 7.2 Hz, 3H). ¹³C NMR (151 MHz, DMSO) δ: 164.4, 149.5, 144.4, 134.8, 132.2, 127.5, 127.3, 123.0, 112.0, 108.3, 52.6, 46.5, 22.1, 19.3, 15.8, 12.0. HRMS (ESI+) *m/z* calcd for C₁₉H₂₁N₅O₂ [M–H][–] 350.1695 found: 350.1612.

4.1.3.26. *N*-hydroxy-4-[(7-ethyl-3-methyl-4,5-dihydropyrazolo[3,4-*e*]indazol-2(7*H*)-yl)methyl]benzamide (A30). Yield: 2.7%. Mp: 204–207 °C. ESI-MS: *m/z*, 350.3 [M–H][–]. ¹H NMR (600 MHz, DMSO-*d*₆) δ: 11.16 (s, 1H), 9.01 (s, 1H), 7.79 (s, 1H), 7.69 (d, *J* = 8.3 Hz, 2H), 7.17 (d, *J* = 8.3 Hz, 2H), 5.28 (s, 2H), 4.07 (q, *J* = 7.2 Hz, 2H), 2.73 (t, *J* = 7.2 Hz, 2H), 2.64 (t, *J* = 7.3 Hz, 2H), 2.14 (s, 3H), 1.36 (t, *J* = 7.3 Hz, 3H). ¹³C NMR (151 MHz, DMSO) δ: 164.4, 149.8, 143.0, 141.6, 134.8, 132.1, 127.5, 127.2, 123.0, 112.5, 111.6, 51.9, 46.4, 22.1, 19.2, 16.0, 9.6. HRMS (ESI+) *m/z* calcd for C₁₉H₂₁N₅O₂ [M–H][–] 350.1695 found: 350.1602.

4.1.3.27. N-hydroxy-4-[(7-(2-methoxyethyl)-3-methyl-4,5-dihydropyr-azolo[3,4-e]indazol-1(7H)-yl)methyl]benzamide (A31). Yield: 0.9%. Mp: 187–190 °C. ESI-MS: m/z , 380.3 [M–H][−]. ¹H NMR (600 MHz, DMSO-*d*₆) δ: 11.07 (s, 1H), 9.03 (s, 1H), 7.90 (s, 1H), 7.67 (d, *J* = 8.1 Hz, 2H), 7.20 (d, *J* = 7.9 Hz, 2H), 5.36 (s, 2H), 4.17 (t, *J* = 5.2 Hz, 2H), 3.65 (t, *J* = 5.2 Hz, 2H), 3.20 (s, 3H), 2.74 (t, *J* = 7.5 Hz, 2H), 2.66 (t, *J* = 7.4 Hz, 2H), 2.10 (s, 3H). ¹³C NMR (151 MHz, DMSO) δ: 171.9, 149.9, 144.4, 134.8, 130.0, 128.6, 127.5, 127.4, 124.4, 124.4, 112.1, 108.4, 70.8, 58.4, 52.7, 51.4, 23.0, 19.3, 12.1. HRMS (ESI+) m/z calcd for C₂₀H₂₃N₅O₃ [M–H][−] 380.1801 found: 380.1720.

4.1.3.28. N-hydroxy-4-[(7-(2-methoxyethyl)-3-methyl-4,5-dihydropyr-azolo[3,4-e]indazol-2(7H)-yl)methyl]benzamide (A32). Yield: 0.8%. Mp: 196–199 °C. ESI-MS: m/z , 380.3 [M–H][−]. ¹H NMR (600 MHz, DMSO-*d*₆) δ: 11.16 (s, 1H), 9.00 (s, 1H), 7.75 (s, 1H), 7.69 (d, *J* = 8.0 Hz, 2H), 7.17 (d, *J* = 8.0 Hz, 2H), 5.29 (s, 2H), 4.20 (t, *J* = 5.2 Hz, 2H), 3.67 (t, *J* = 5.2 Hz, 2H), 3.24 (s, 3H), 2.73 (t, *J* = 7.2 Hz, 2H), 2.65 (t, *J* = 7.2 Hz, 2H), 2.14 (s, 3H). ¹³C NMR (151 MHz, DMSO) δ: 164.5, 150.1, 142.8, 141.6, 134.9, 132.1, 127.5, 127.2, 124.2, 112.6, 111.6, 70.9, 58.3, 51.9, 51.2, 22.1, 19.1, 9.6. HRMS (ESI+) m/z calcd for C₂₀H₂₃N₅O₃ [M–H][−] 380.1801 found: 380.1702.

4.1.3.29. N-hydroxy-4-[(6-(2-methoxyethyl)-3-methyl-4,5-dihydropyr-azolo[3,4-e]indazol-1(6H)-yl)methyl]benzamide (A33). Yield: 0.5%. Mp: 176–179 °C. ESI-MS: m/z , 379.6 [M–H][−]. ¹H NMR (600 MHz, DMSO-*d*₆) δ: 11.14 (s, 1H), 8.98 (s, 1H), 7.90 (s, 1H), 7.68–7.65 (m, 2H), 7.21 (t, *J* = 8.1 Hz, 2H), 5.36 (s, 2H), 4.17 (t, *J* = 5.3 Hz, 2H), 3.65 (t, *J* = 5.3 Hz, 2H), 3.19 (s, 3H), 2.74 (t, *J* = 7.5 Hz, 2H), 2.66 (t, *J* = 7.5 Hz, 2H), 2.10 (s, 3H). ¹³C NMR (151 MHz, DMSO) δ: 164.4, 149.8, 144.5, 134.7, 132.1, 127.6, 127.4, 127.3, 124.3, 112.2, 110.6, 108.4, 70.8, 58.4, 52.7, 51.4, 22.2, 19.3, 12.1. LC-MS m/z 379.6 [M–H][−].

4.1.3.30. N-hydroxy-4-[(6-(2-methoxyethyl)-3-methyl-4,5-dihydropyr-azolo[3,4-e]indazol-2(6H)-yl)methyl]benzamide (A34). Yield: 0.6%. Mp: 181–183 °C. ESI-MS: m/z , 379.6 [M–H][−]. ¹H NMR (600 MHz, DMSO-*d*₆) δ: 11.15 (s, 1H), 9.00 (s, 1H), 7.69 (d, *J* = 8.0 Hz, 2H), 7.53 (s, 1H), 7.17 (d, *J* = 8.0 Hz, 2H), 5.28 (s, 2H), 4.22 (t, *J* = 5.3 Hz, 2H), 3.64 (t, *J* = 5.3 Hz, 2H), 3.20 (s, 3H), 2.86 (t, *J* = 7.6 Hz, 2H), 2.68 (t, *J* = 7.6 Hz, 2H), 2.14 (s, 3H). ¹³C NMR (151 MHz, DMSO) δ: 164.5, 150.4, 143.4, 141.8, 134.7, 132.4, 127.6, 127.2, 124.2, 112.4, 111.3, 71.3, 58.6, 51.9, 48.9, 20.6, 18.9, 9.8. LC-MS m/z 379.6 [M–H][−].

4.2. Biological assays

4.2.1. Cell culture

The mouse N9 microglial cultures were placed into IMDM medium supplemented 5% FBS for 24 h. PC12 cells were maintained in RPMI1640 supplemented with 10% FBS, 100 units/ml Penicillin G and 100 g/ml streptomycin. All the cells were incubated at 37 °C in humidified air containing with 5% CO₂.

4.2.2. HDAC inhibition assay

The general procedure for the enzyme-based assay was carried out according to published protocols [24] with slight modification. The recombinant human HDAC1, 2, 3 and 6 were purchased from BPS Bioscience (USA). All reactions were performed in the black half area 96-well plates. A serial dilution of the inhibitors (5 μL/well) and enzymes (5 μL/well) were pre-incubated in HDAC buffer (10 μL/well) at 25 °C for 15 min, then fluorogenic substrate (5 μL/well) Boc-Lys(Ac)-AMC was added. After incubation at 37 °C for 60 min, the mixture was stopped by the addition of developer (25 μL/well) for 10 min. Fluorescence intensity was measured using the Thermo Scientific Varioskan Flash Station at excitation and emission wavelengths of 355 and 460 nm, respectively. The IC₅₀ values were extracted by curve fitting the dose/response slopes. The IC₅₀ values were the mean of two independent

determinations.

4.2.3. Nitrite determination assay

N9 cells were incubated for 24 h by adherent culture. Cells were incubated with 1 μg/ml LPS (Sigma-Aldrich) and different concentrations (0.01 μM, 0.1 μM, 1 μM and 10 μM) of compounds in serum-free medium for 24 h. Nitrite concentration (as a measure of NO production) in the supernatant was determined by using Griess reagents. The absorbance was measured at 540 nm using a microplate reader (Synergy-HT, Biotek). The IC₅₀ values were the mean of two independent determinations.

4.2.4. NO capture ability determination assay

SNP (Sodium Nitroprusside) was dissolved in PBS to prepare the 100 mM stock solution. In this experiment, SNP solution of 25 μL was added to 975 μL PBS solution which included different concentration of tested compounds. After 60 min under room temperature condition, the concentration of NO^{2−} was tested using Griess assay. The inhibitions of serial concentrations of compounds were calculated and the IC₅₀ were estimated using Logit method. The data (mean ± SD) were calculated according to inhibition ratios from three independent tests.

4.2.5. Western blot assay

The human neuroblastoma cell line SH-SY5Y cells were incubated in presence of the test compound A16 and Tubacin (in 0.5% DMSO) for 12 h, harvested, and rinsed with ice-cold PBS. Total protein extracts (40 μg) were prepared by lysing cells in NP40 buffer (50 mM Tris-HCl, pH 8.0 0.5% sodium deoxycholate, 100 μM leupeptin, 2 μg/mL aprotinin, 150 mM NaCl, 1% NP-40, 0.1% SDS and 1 mM phenylmethylsulfonyl fluoride). Protein concentrations in the lysates were determined using a Bio-Rad protein assay kit (Bio-Rad Laboratories Inc., Hercules, CA, USA) according to the manufacturer's instructions. The samples were separated on SDS polyacrylamide gels and then transferred to nitrocellulose membranes and blocked with 5% nonfat dried milk. The membranes were incubated with antibodies to H3, Ac-H3, α-tubulin, Ac-tubulin, HDAC6, and β-actin overnight at 4 °C. The immune-complexes were visualized using enhanced chemiluminescence western blot detection reagents (Amersham Biosciences Inc., Piscataway, NJ).

4.2.6. Evaluation of inflammatory mediator assay

The secreted levels of TNF and IL-6 were measured using Mouse Th1/Th2/Th17 Cytokine Kit. It was purchased from BD Pharmingen. After specific time in the LPS condition, the supernatants were collected and analyzed by a flow cytometer (BD FACSCalibur). The data was analyzed by FCAP Array v3.0. IL-2, IL-4, IL-10, IL-17A and IFN-γ were not detected in the experiment. The data (mean ± SD) were calculated according to inhibition ratios from three independent tests.

4.2.7. MTT assay

N9 Cells were seeded in 96-well plates at 50 × 10⁴/ml (100 μL/well). After 24 h incubation, 4 different concentrations (final concentrations were 0.01, 0.1, 1 and 10 μM) of tested compounds were added into the wells. Cells were incubated for the continuous 24 h. After treatment, MTT was added into the cells at a final concentration of 500 μg/ml, and the plates were incubated for an additional 4 h. The resultant formazan crystals were dissolved in 200 μL of DMSO, and the absorbance was measured at 570 nm using a microplate reader (Synergy HT, Bio-Tek). The data (mean ± SD) were calculated according to inhibition ratios from three independent tests.

4.2.8. The protection of A16 on H₂O₂-induced PC12 injury assay

MTT assay was used to determine the cell viability. PC12 cells were seeded at 20 × 10⁴/ml (100 μL/well) in 96-well plate. After 24 h, cells were pretreated with A16 and ACY-1215 for 1 h, and then challenge H₂O₂ (500 μM) and incubated for 16 h. Cells were added with 5 mg/ml MTT and incubated for additional 4 h. The optimal density was detected

by the microplate reader at a wavelength of 570 nm. The data (mean \pm SD) were calculated according to inhibition ratios from three independent tests.

4.2.9. DPPH scavenging capacity assay

The radical scavenging activity of compounds was determined by using DPPH assay. In the experiment, a DPPH ethanol solution with a concentration of 1×10^{-4} M was prepared, and placed on a shaker away from light for 30 min. The volume of 100 μ L of each concentration of the medicinal solution was pipetted, and 900 μ L of a 1×10^{-4} M DPPH ethanol solution was added. After shaking, it was left at room temperature for 60 min. The absorbance at 517 nm was detected by a microplate reader. The data (mean \pm SD) were calculated according to inhibition ratios from three independent tests.

4.2.10. Acute toxicity assay

Experiments were carried out on male adult Kuming mice (18–22 g) were purchased from Experimental Animal Center of Shenyang pharmaceutical University. All procedures were approved by the Animal Care Committee at Shenyang pharmaceutical University. The mice were acclimatized to the laboratory for at least 3 days before starting experiments. The mice were housed at five per cage in cages with a 12-hr light/dark cycle and had free access to food and water under controlled temperature (20–24 °C) and humidity (45–65%). Food and water were allowed ad libitum during the study period. A total of 15 male adult Kuming mice were randomly divided in 5 groups with 3 animals. Before the administration of different doses of formulation, the mice were fasted for 16 h with water ad libitum. The mice were given 1000, 500, 250, 125, 62.5 mg/kg of A16 with a intraperitoneal injection. Then, the animals were continuously observed during the first 1 h for the general behavior and signs of toxicity, then intermittently observed for 4 h, and thereafter over a period of 24 h. The animals were observed daily in continuous 7 days. The median lethal dose (LD₅₀) calculated through mortality and the survival rates by Bliss method.

4.2.11. The stability assay

Two species liver microsomes were diluted with 0.1 M potassium phosphate buffer, 3 mM MgCl₂ to a final protein concentration of 0.5 mg/mL. The microsomes were incubated with compound (1 μ M) in the presence of NADPH system at 37 °C. The samples were taken for 0, 5, 10, 20, 30, 60 min and quenched with acetonitrile, followed by vortexed for 3 min and centrifuged at 13000 rpm for 10 min. The content of compound in the supernatants was determined by LC-MS/MS analysis, and its half-time ($T_{1/2}$) and intrinsic clearance rate (CL_{int}) was calculated. The experiments were performed twice parallelly, and the results were presented as mean.

The rat plasma was incubated with compound (1 μ M) at 37 °C. The sample was taken at the indicated time points during the incubation (0, 10, 20, 30, 60, and 120 min). The reactions terminated with the addition of 4 volumes of cold acetonitrile containing an internal standard. The concentrations of remaining compound were analyzed by LC-MS/MS. The experiments were performed twice parallelly, and the results were presented as mean.

4.2.12. Statistical analysis

Statistics datum were presented as mean \pm SD and representative of at least three independent trials. Multiple-group comparisons were performed using a one-way ANOVA followed by Dunnett's *t*-test. Two group comparisons were performed using Student's *t*-test. A *p* < 0.05 was considered statistically significant.

Declaration of Competing Interest

The authors declare that they have no known competing financial interests or personal relationships that could have appeared to influence the work reported in this paper.

Acknowledgement

This work was supported by the National Natural Science Foundation of China (No.81473086), the Natural Science Foundation of Liaoning Province, China (No.2015020728-301) and LiaoNing - Revitalization Talents Program (XLYC1902089).

References

- [1] P. Bjerling, R.A. Silverstein, G. Thon, et al., Functional divergence between histone deacetylases in fission yeast by distinct cellular localization and in vivo specificity, *Mol. Cell. Biol.* 22 (2002) 2170–2181.
- [2] W. Fischle, F. Dequiedt, M.J. Hendzel, et al., Enzymatic activity associated with class II HDACs is dependent on a multiprotein complex containing HDAC3 and SMRT/N-CoR, *Mol. Cell* 9 (2002) 45–57.
- [3] S. Demyanenko, V. Dzreyan, A. Uzdensky, Overexpression of HDAC6, but not HDAC3 and HDAC4 in the penumbra after photothrombotic stroke in the rat cerebral cortex and the neuroprotective effects of α -phenyl tropolone, HPOB, and sodium valproate, *Brain Res. Bull.* 162 (2020) 151–165.
- [4] Z. Wang, Y. Leng, J. Wang, et al., Tubastatin A, an HDAC6 inhibitor, alleviates stroke-induced brain infarction and functional deficits: potential roles of α -tubulin acetylation and FGF-21 up-regulation, *Sci. Rep.* 6 (2016) 19626.
- [5] M.A. Rivieccio, C. Brochier, D.E. Willis, et al., HDAC6 is a target for protection and regeneration following injury in the nervous system, *Proc. Natl. Acad. Sci. USA* 106 (2009) 19599–19604.
- [6] X. Xu, A.P. Kozikowski, L. Pozzo-Miller, A selective histone deacetylase-6 inhibitor improves BDNF trafficking in hippocampal neurons from Mecp2 knockout mice: implications for Rett syndrome, *Front. Cell Neurosci.* 8 (2014) 68.
- [7] S. Dallavalle, C. Pisano, F. Zunino, Development and therapeutic impact of HDAC6-selective inhibitors, *Biochem. Pharmacol.* 84 (2012) 756–765.
- [8] L. Santo, T. Hideshima, A.L. Kung, et al., Preclinical activity, pharmacodynamic, and pharmacokinetic properties of a selective HDAC6 inhibitor, ACY-1215, in combination with bortezomib in multiple myeloma, *Blood* 119 (2012) 2579–2589.
- [9] A.J. Yee, W.I. Bensinger, J.G. Supko, et al., Ricolinostat plus lenalidomide, and dexamethasone in relapsed or refractory multiple myeloma: a multicentre phase 1b trial, *Lancet Oncol.* 17 (2016) 1569–1578.
- [10] P. Huang, I. Almeciga-Pinto, M. Jarpe, et al., Selective HDAC inhibition by ACY-241 enhances the activity of paclitaxel in solid tumor model, *Oncotarget.* 8 (2015) 2694.
- [11] R. Niesvizky, P.G. Richardson, N.Y. Gabrail et al., ACY-241, a novel, HDAC6 selective inhibitor: Synergy with immunomodulatory (IMiD) drugs in multiple myeloma (MM) cells and early clinical results (ACE-MM-200 Study), 57th Annu Meet Am Soc Hematol (December 5–8, Orlando) 2015, Abstr 3040.
- [12] J. Stephen, Shuttleworth, KA2237 and KA2507: Novel, oral cancer immunotherapeutics targeting PI3K-p110 β /p110 δ and HDAC6 with single-agent and combination activity, in: Proceedings of the 107th Annual Meeting of the American Association for Cancer Research; 2016 Apr 16–20; New Orleans, LA. Philadelphia (PA): AACR; Cancer Res 2016, 76(14 Suppl): Abstract nr 3996.
- [13] M. Brindisi, A.P. Saraswati, S. Brogi, et al., Old but Gold: Tracking the New Guise of Histone Deacetylase 6 (HDAC6) Enzyme as a Biomarker and Therapeutic Target in Rare Diseases, *J. Med. Chem.* 63 (2020) 23–39.
- [14] Yuanjian Song, Li Qin, Rongli Yang, et al., Inhibition of HDAC6 alleviating lipopolysaccharide-induced p38MAPK phosphorylation and neuroinflammation in mice, *Pharm. Biol.* 57 (2019) 263–268.
- [15] M.G. Olga, M. Federico, S.M. Francisco, HDAC6 at Crossroads of Infection and Innate Immunity, *Trends Immunol.* 39 (2018) 591–595.
- [16] Lin Li, Xiangjiao Yang, Tubulin acetylation: responsible enzymes, biological functions and human diseases, *Cell. Mol. Life Sci.* 72 (2015) 4237–4255.
- [17] J. Yang, G. Cheng, Q. Xu, et al., Design, synthesis and biological evaluation of novel hydroxamic acid based histone deacetylase 6 selective inhibitors bearing phenylpyrazol scaffold as surface recognition motif, *Bioorg. Med. Chem.* 26 (2018) 1418–1425.
- [18] R. Jin, G. Yang, G. Li, Inflammatory mechanisms in ischemic stroke: role of inflammatory cells, *J. Leukoc. Biol.* 87 (2010) 779–789.
- [19] Y. Chen, J.M. Hallenbeck, C. Ruetzler, et al., Overexpression of monocyte chemoattractant protein 1 in the brain exacerbates ischemic brain injury and is associated with recruitment of inflammatory cells, *J. Cereb. Blood Flow Metab.* 23 (2003) 748–755.
- [20] M. Gliem, A.K. Mausberg, J.I. Lee, et al., Macrophages prevent hemorrhagic infarct transformation in murine stroke models, *Ann. Neurol.* 71 (2012) 743–752.
- [21] J. Zhang, X. Fang, Y. Zhou, et al., The Possible Damaged Mechanism and the Preventive Effect of Monosialotetrahexosylganglioside in a rat Model of Cerebral Ischemia-Reperfusion Injury, *J. Stroke Cerebrovasc. Dis.* 24 (2015) 1471–1478.
- [22] A. Ozkul, A. Akyol, C. Yenisey, et al., Oxidative stress in acute ischemic stroke, *J. Clin. Neurosci.* 14 (2007) 1062–1066.
- [23] P. Liu, H. Zhao, R. Wang, et al., Micro RNA-424 protects against focal cerebral ischemia and reperfusion injury in mice by suppressing oxidative stress, *Stroke* 46 (2015) 513–519.
- [24] F.W. Dennis Wegener, Daniel Riester, Andreas Schwienhorst, A fluorogenic histone deacetylase assay well suited for high-throughput activity screening, *Chem. Biol.* 10 (2003), 61–68.